European Commission

JRC SCIENTIFIC AND POLICY REPORTS

Objective 2: Conduct Experimental Activities on Performance of Sensor-Equipped Composite Elements

Deliverable 02.02: Evaluate physical performance of embedded sensor systems.

N.A. Chrysochoidis, S. Mainetti, E. Ruotolo, E. Gutiérrez (DG JRC)

2013

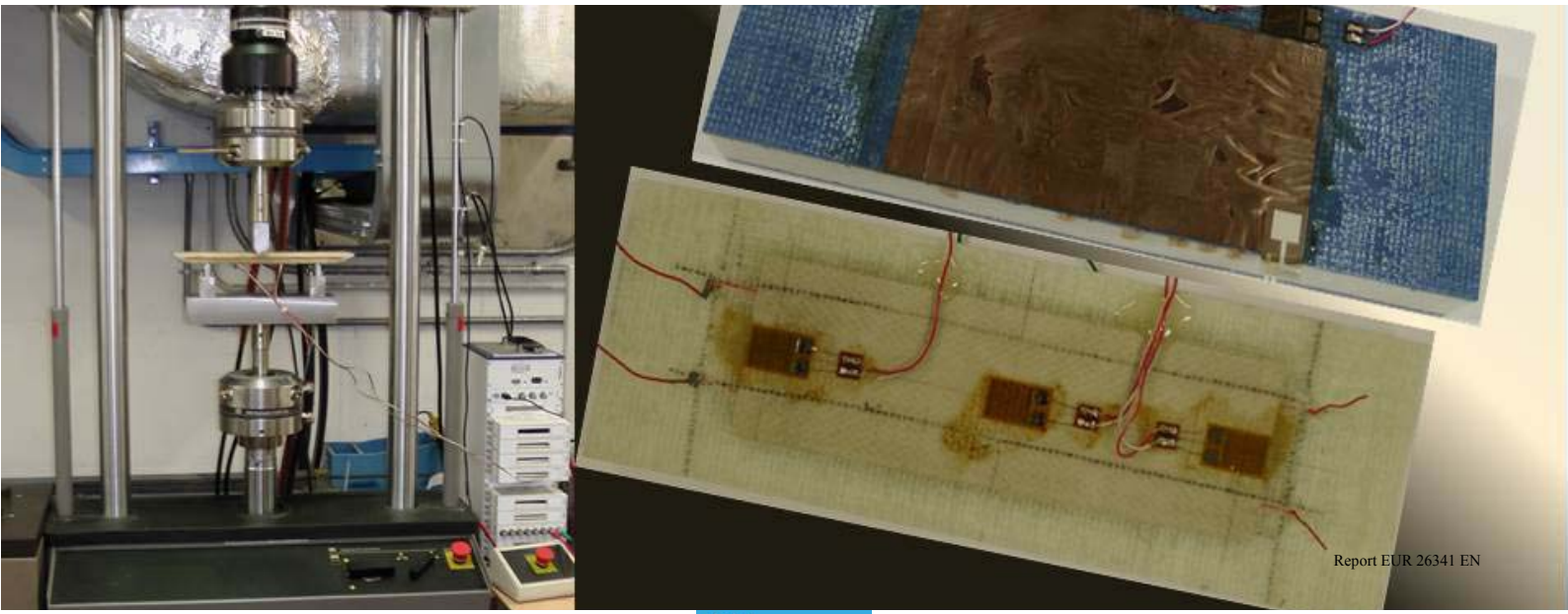

Report EUR 26341 EN

Joint Research Centre

European Commission
Joint Research Centre
Institute for Protection and Security of the Citizen

Contact information
Eugenio Gutiérrez
Address: Joint Research Centre, Via Enrico Fermi 2749, TP 480, 21027 Ispra (VA), Italy
E-mail: eugenio.gutierrez@jrc.ec.europa.eu
Tel.: +39 0332 78 5711
Fax: +30 0332 78 9049

http://ipsc.jrc.ec.europa.eu/
http://www.jrc.ec.europa.eu/

JRC85593

EUR 26341 EN

ISBN 978-92-79-34691-0

ISSN 1831-9424

doi:10.2788/41247

Luxembourg: Publications Office of the European Union, 2013

Printed in Italy

Deliverable Administration & Summary		**STEC**			**41999**
No & name	D02.02 Evaluate physical performance of embedded sensor systems				
Status	Final	**Due**	July 2013	Date	November 2013
Author(s)	N.A. Chrysochoidis, S. Mainetti, E. Ruotolo, E.Gutiérrez (DG-JRC Unit G05)				

Contents

FIGURES

TABLES

Summary

We present the preliminary results of our production trials and experimental research campaign for embedding sensors and energy-harvesting devices in sandwich composite structures that would also form the primary structural component of so-called, smart tamper-evident shipping containers.

To develop an embedded energy-autonomous structural and anti-tamper monitoring system, it is first required to introduce a sensor unobtrusively within the material of which the structure is made of. Then it is required to ensure that the sensor and the communication system are equipped with enough energy to keep the system active as long as necessary.

This report first describes how to combine a class of self-energizing piezo-polymers within fibre-reinforced composites by introducing them between the layers of the composite laminate using the resin infusion manufacturing method. This is followed by a description of the calibration procedure of the embedded systems, their energy-harvesting capacity and strain sensitivity.

We conclude with some observations regarding the nature of the bond at the interface between the sensors and the parent material, and how these may depend on the nature of the conductive inks and films used to generate the electrode surfaces of the piezo-sensors.

1. Introduction

One of the objectives of the STEC action is to develop a class of communication systems whereby a shipping container would be capable of broadcasting to some receiver its functional status. This 'functional status' could perhaps inform the end users (a customs agency, shipper or relevant stakeholder) of the temperature inside the container, its structural or security integrity or some other diagnostic.
It has also been suggested that by using fibre-reinforced composites as one of the primary load-bearing materials, it would be possible not only to reduce weight but also to embed sensors within the structure itself, thus acting as; so-called, 'smart structures'. A key criterion of the design process of such systems is that, given the fact that containers (for a number of reasons) are deprived of a reliable energy source, the electronic devices required to maintain such a diagnostic system would have to rely on a limited energy supply (batteries), and would therefore have to have either very low power consumption or ideally, be capable of scavenging the required energy from their immediate environments.
If the sensor is itself embedded into the lamination of a fibre-reinforced composite, then it becomes of primary importance to identify the most suitable location for the

placement of such devices in order to for optimize their energy-harvesting and structural metrology capacities.

One of the most advantageous aspects of piezoelectric devices is that they can provide a reliable and continuous two-way energy conversion between dynamic strain and electrical energy without the need of an external power supply; piezo materials, therefore, can be used both as energy harvesters and strain gauges. Herein we report on an experimental study of the efficiency of piezopolymer (PVDF) films to satisfy the requirement of providing both energy-harvesting and self-energizing capabilities for composite embedded sensors and their associated microcontrollers and wireless transduction devices.

Given the economic constraints of the shipping container industry, this type of sensor should combine low cost (making them attractive for other requisites of the shipping container industry) and potentially high sensitivity; all in all: to provide the required electrical energy for the detection, data acquisition, processing and broadcasting systems.

Embedding these sensors in a shipping container requires selecting an area where they remain protected, and yet provide the conditions for the sensors to operate to their maximum possible performance. One solution can be the insertion of these devices through the thickness of the composite laminate during the composite manufacturing procedure. In this sense, the thinness (~30μm) of the piezopolymer material makes them more attractive for embedding applications than standard piezo-ceramics, which are usually much thicker(~1-2mm) and brittle. However, even in spite of their thinness, the drawback is that the insertion of an artifact in the composite laminate entails the possibility of artificially creating a damage zone (more specifically a delamination or de-bonding interface), which could have a significant impact on the structural performance of both the sensor and the host structure. To this end, the placement of an embedded device should offer a balance between the two requirements of sensor efficiency and the structural performance of the composite structure.

In this document, as well as describing the manufacturing procedure of sensor-embedded composite laminates, we also report on the investigations on the performance-varying geometry of said devices that could either be used to measure strains and/or harvest strain energy. To quantify the device performance the sensitivity is measured under various setups and placement configurations. The scope of the investigations is therefore to examine how piezopolymer devices operate as electromechanical energy transducers, and, more specifically, how their sensitivity relates to the average strain generated across the area they span.

Another aspect presented in this report concerns the manner in which the PVDF films are placed on or into the composite specimens; thus, we shall also present a number of supra and intra-laminar bonding methods on a wide variety of candidate materials ranging from bonding sensors, to simple laminates using cyanoacrylate glues, to vacuum-assisted embedded systems in sandwich panels.

2. Current State of Art

Piezoelectrics (piezopolymer and piezoceramics) are one of the most promising actuator/sensor devices which can be either bonded onto the surface of a structure or embedded within it. The integration of diagnostic devices in a component depends upon the requirements of the, so called, 'smart' structure. Laminated fiber reinforced composites are one of the most preferred host materials for smart structures due to the ease of embedment of the sensors and/or actuators and their inherent advantages as structural materials. The bulk of the scientific literature in the area of embedding sensors in a composite laminate focuses on the effect on the host to its global structural performance.

Embedding of smart devices within composite laminates is a research area that has been increasingly studied over the last two decades. Various aspects have been examined, such as the methods of embedding an actuator/sensor in the composite laminate, the appropriate type of sensor, as well as their static and fatigue performance. These studies have dealt with embedding various types of sensors such as piezopolymers, fiber optics, shape memory alloys, strain sensors, and, more recently, the potential of creating a smart matrix system based on the usage of nanoparticles. Herein, our study focuses only on the use of polymer piezoelectric devices. Among the various methodologies of embedding sensors, there are two approaches:

(i) Some researchers have chosen to cut the plies surrounding the embedded device ([1] [2] [3] [4], [5] [6]), which is usually performed when the device is thick (~1-2 mm) like a piezoceramic patch.
(ii) The second manufacturing approach is based on the direct placement of the sensor in the laminate between the plies without any cut-outs.

The embedded device in a composite structure would generally cause a discontinuity that could result in a significant effect on the structural integrity. In this case, the placement of the sensor was considered as an inclusion that not only results in the net area loss of the material, but additional interlaminar stresses may also arise at, or near, the discontinuity within the host composite structure; this may result in a reduction of the load-carrying capability.

Other studies investigated the potential of embedding piezopolymer sensors having different characteristics and applications. Bellan et al [9] embedded special piezopolymer films for the propagation of high frequency Lamb waves. A research group from Stanford University [10] developed a commercial transducer called the Stanford Multi- Actuator Receiver Transduction layer (SMART Layer). This transducer could be customized in a variety of sizes, shapes and complexity, allowing its embedding into many composite structures such as pressure vessels, pipes or wings.

One critical aspect of embedding sensors concerns the generated interlaminar stresses at the interface between sensor/actuator and the host structure, which can result in debonding. In this case, the embedded device may lose the ability to perform its role in

the adaptive structure or, alternatively, the embedded device itself may fail (break). To this end, two aspects of the structural performance were further investigated in the literature: the static and the fatigue structural performance.

These factors have motivated the following studies:

Warkentin and Crawley [4] investigated the graphite/epoxy coupons embedded with integrated circuits on silicon chips. Their results showed a reduction of 15% in the ultimate strength of host laminate due to the presence of embedded semiconductor chips.

Investigations by Crawley and de Luis [11] showed that the ultimate strength of a glass/epoxy laminate was reduced by 20% when piezoceramic was embedded in the composite.

Chow and Graves investigated analytically the case of embedded-device laminates [12]. Simulations showed that interlaminar stresses resulting from the embedding of an inert rectangular implant in a graphite/epoxy laminate increased by about five times in magnitude, thus showing that the integrity of smart structures could be affected due to insertion of sensor/actuators.

Vizzini and his colleagues [5], [6] have developed a manufacturing technique to reduce the interlaminar stress by distributing the discontinuity through the laminate thickness and investigated its performance experimentally and analytically using finite elements. This technique, referred to as interlacing the embedded sensor/actuator, is similar to the ply drop-off technique. The analytical predictions as well as the experimental measurements were significantly encouraging as they recorded an increase in the structural performance by a factor of two. Additionally, the fatigue performance of the structure with embedded devices using this special technique was studied, concluding that the onset of damage was delayed and the progression of delamination was impeded.

As regards embedding piezopolymers, Caneva et al [13] presented a study of investigating the structural integrity using Acoustic Emission (AE) of Aramid/Epoxy composite strips subjected to quasistatic three point bending. These specimens were integrated with attached or embedded small piezopolymer sensors, which additionally were used as acoustic emission sensors. Flexural moduli as well as the strength of the specimens were recorded and they were slightly affected due to the presence of sensors. Additionally the AE history recorded indicated small differences, mainly related to the nature of incidents received by the sensor due to its location on or inside the structure.

The Composite Structures and Materials group from the EMPA Swiss Federal Laboratories [14], present an alternative study for the structural performance of Glass/Epoxy laminates with embedded custom made MFC (Macro-Fiber Composites) and AFC sensors under pre-stressed configuration. The tested structure was loaded and unloaded until a specific threshold and the structural integrity was measured using Acoustic Emission. Results showed an increased performance of the composite structure when the sensor was integrated in the laminate.

Concerning the structural fatigue performance, the bulk of the literature has so far concentrated on the investigation of the electromechanical fatigue of composite laminates with embedded piezoceramic devices operating as actuators and sensors. Additionally, a question appears concerning the justification of the performance of a structure with an embedded sensor/actuator: is the ultimate fatigue performance a function of the material or is there a perturbation introduced by the sensor itself?

Bronowicki et al [15] tested graphite/epoxy composites equipped with embedded active PZT (lead zirconium titanate). These laminates were loaded to external tensile mechanical load, and then unloaded completely. Thereafter, the embedded PZTs were excited by the external voltage to evaluate their actuation capability by measuring the strain on the surface of the laminate. The PZTs were found to be almost unchanged following the application of external loads.

Mall and Coleman investigated the effects of embedded active PZT sensor/actuators on the tensile strength and fatigue behavior of quasi-isotropic graphite/epoxy laminates [16]. For this purpose they used a widely available lamination used in aerospace applications and a PZT in pre-packed form with extended lead wires inserted into a cutout area into the two middle 90° plies. Monotonic tensile tests showed that both the average ultimate strength and Young's modulus of this laminate with or without PZT were within 4% of each other. Mechanical fatigue tests were also conducted with specimens without or with embedded PZTs under mechanical cyclic loading conditions. These tests were conducted to establish the fatigue life diagram (SN curves), which illustrated that the fatigue lifetimes of this laminate with and without PZT were compatible. On the other hand, the voltage output of the embedded PZT degraded sharply after the first cycle of fatigue loading. More recent works of Mall and coworkers [17] studied the combined electromechanical fatigue behavior of the composites structure with the embedded actuation/sensing devices. These studies indicated that the measured fatigue life was drastically affected for the case where the applied mechanical and the electrical cyclic fatigue loading were in and out of phase.

Subsequently, Tang et al [18] have used embedded piezoceramic devices to investigate the structural integrity of laminated composites subjected to fatigue loading. More specifically, an experimental setup, performed by embedded piezoceramic actuator/sensor pairs was used to measure the degradation on the structural performance via modifications on the propagated stress wave characteristics resulting from the presence of damage in the tested laminate (the "pitch and catch" technique).

Additionally, Schaaf et al [19] have studied the performance of unidirectional composite laminates under three point bending for static and fatigue loading. The tested specimens contained miniature chip resistors simulating the embedded sensors or PVDF sensors. The objective of their study was the experimental investigation of the interlaminar stresses generated at the interfaces of the embedded sensors systems as well as the composite specimens' structural integrity. Results indicated a drastic reduction of the structural performance, especially in the case where the embedded device was a PVDF film. Another work of the same group [20] addresses the tension performance of various laminations of Glass/Epoxy composite strips integrated with

miniature chip resistors simulating a dummy embedded sensor. During testing, acoustic emission history was recorded indicating the presence of early events during loading related with matrix cracking due to the presence of the embedded device.

The object of our study is to extend the present literature by providing further results relating to experimental methods for embedding sensors and, more specifically, to investigate the quasistatic and cyclic performance of composite laminates with and without embedded devices. A key objective is to identify the optimum positions for the sensors' placement in order to have them well protected and to provide the maximum electrical energy for energy harvesting applications. This study is also a follow up to [19] and focuses on the application of piezopolymer sensors in the composite laminate structures (beam/ panels).

Future experimental campaigns will focus on comparing the static performance of composite sandwich panels with and without a host presence according to the ASTM standards. A second aspect will investigate the fatigue performance on the reduction of the sensor voltage and the sensor capacitance as well as the structural integrity.

3. Materials and Sensors

The specimens tested were all fabricated in-house at the ELSA laboratory. The fabricated specimens were:

1. Flat composite panels for the extraction of the properties of the tested composite laminates.
2. Composite strips with embedded piezopolymer sensors.
3. Meso scale sandwich composite panels with and without embedded piezopolymer sensors.

For the fabrication of the composite laminate we used the vacuum-assisted resin infusion methodology; more specifically layers of 0/90 fabric cloth (205g/m^2) infused with epoxy resin. Fiberglass woven reinforcement was chosen for two reasons: (1) because of the transparency of the cured material, the ability to visually track the transducers in the specimens and (2) as fiberglass is nonconductive, the ease of electrically wiring the transducers located inside the plates. The specifications of the cured epoxy resin are illustrated in Table 1 given by the material producer [22].

For the core of the sandwich composite structure two different materials were tried: commercially available plywood and expanded foam. The first prototype was conducted using common plywood panels in order to validate the resin system, the resin flow mesh and the feasibility of embedding PDVF films (folded and otherwise) during the vacuum-assisted molding. Properties of the plywood core aren't provided, but the foam core used was the AIREX 92.90 with properties given inTable 2.

We used a variety of piezopolymer device formats but in all cases the piezo material was poled PVDF (Polyvinylidene fluoride). In some cases the sensors were placed within the thickness of the composite laminate, i.e., between two successive

composite plies, while others were attached on the exterior composite laminate surface. The electromechanical properties of the PVDFs used are summarized in Table 3 as provided by the manufacturer (Measurement Specialties).

The various shapes of piezopolymers used for the specimen fabrication are illustrated in Figure 1 to Figure 5 providing also the main geometrical details. The electromechanical transduction can be calculated according to the equation: $V = k_p s;$ where $k_p = g_{31} Y t$; where the material constants shown are taken from the tables above, and t is the thickness of the PVDF film [19]. Using this equation the sensitivity of the sensors used in our experiments is expected to be in the range 41 to 82.6 micro-strain/Volt. This value was calculated for a sensor with thickness 28μm assuming $g_{31} \approx 0.216 Vm/N; Y = 2-4 GPa.$

Table 1 Properties of Epoxy Resin.

Property	Method	Units	AT30 SLOW	AT30 FAST
Colour			Pale yellow	Pale yellow
Machinability			Excellent	Excellent
Density 25°C	ASTM D 792	g/ml	1.08 – 1.12	1.08 – 1.12
Hardness 25°C	ASTM D 2240	Shore D/15	84.5 – 88.5	86 – 90
Maximum Tg	ASTM D 3418	°C	92 – 98	75 – 81
Water absorption (24h RT)	ASTM D 570	%	0.12 – 0.20	0.22 – 0.27
Water absorption (2hr 100°C)	ASTM D 570	%	0.58 – 0.70	0.95 – 1.00
Flexural strength	ASTM D 790)	MN/m²	112 – 124	95 – 109
Maximum strain	ASTM D 790)	%	5 – 7	4 – 6
Strain at break	ASTM D 790)	%	6 – 8	7 – 9
Flexural modulus	ASTM D 790)	MN/m²	3.15 – 3.55	2.5 – 3.1
Tensile strength	ASTM D 638	MN/m²	65.5 – 73.5	67.0 – 75.0
Elongation at break	ASTM D 638	%	6 – 8	5 – 7

Table 2 Properties of the AIREX[1] T92.90 core material.

Density	Kg/m^3	85
Compressive Strength	MPa	1.0
Compressive Modulus	MPa	70
Tensile strength	MPa	1.5
Tensile Modulus	MPa	90
Shear Strength	MPa	0.65
Shear Modulus	MPa	17

[1] Core material coupons provided by AIREX

Table 3 Electromechanical Properties of used PVDF Materials.

Young's Modulus (Y)	GPa	2-4
Yield Strength	MPa	45-55
Relative Permittivity ($\varepsilon/\varepsilon_0$)		12
d_{31} (charge mode piezoelectric coefficient)	C/N	23 x 10^{-12}
g_{31} (voltage mode piezoelectric coefficient)	Vm/N	216 x 10^{-3}
Pyroelectric Coefficient	C/^{o}K m^2	30 x 10^{-6}
Density	Kg/m^3	1780

1st Type : Metallized Piezo Film

Nominal Capacitance: 85 nF
***Part number: 1-1004347-0 Model Description: Metalized Piezo Films* [21]**

Figure 1. Sensor Type 1

2nd Type : Custom made Metallized Piezo Film with Terminals

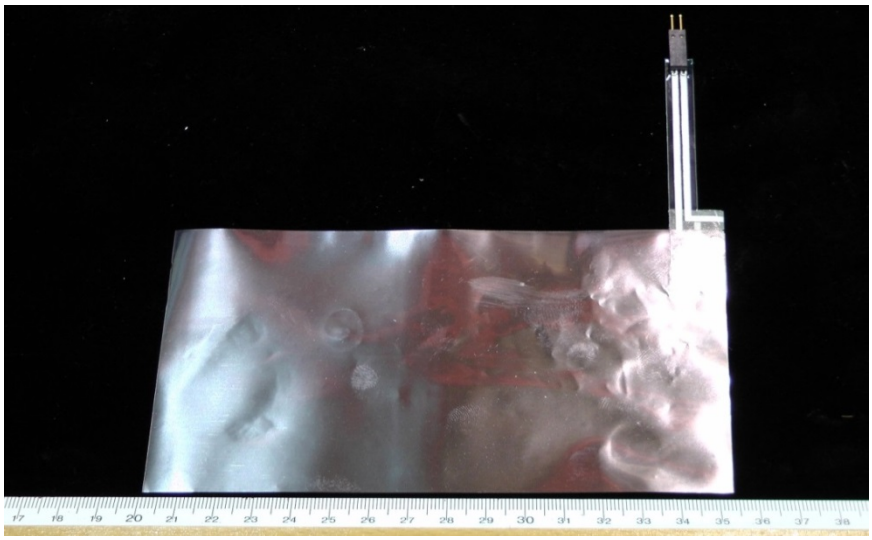

Manufacturer Description: Audio Speaker Element
NiCu Metallization, Thickness: 56μm, Length:152mm , Width:79mm ,Nominal Capacitance: 44nF [21]

Figure 2. Sensor Type 2

3rd Type : Thin Piezo Film without plastic cover

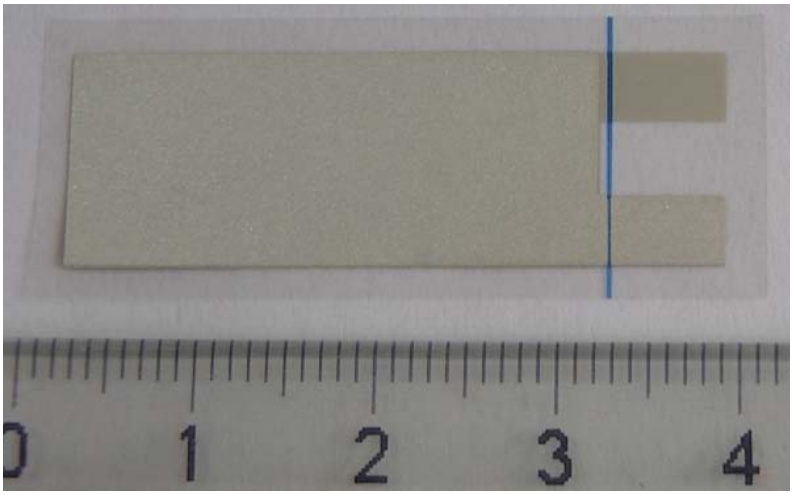

Nominal Capacitance: 1.35 nF
Part number: 1-1002608-0 Model Description:DT1-028K [21]

Figure 3. Sensor Type 3

4th Type : Piezo Film with Mylar cover and silver ink screen printed electrodes

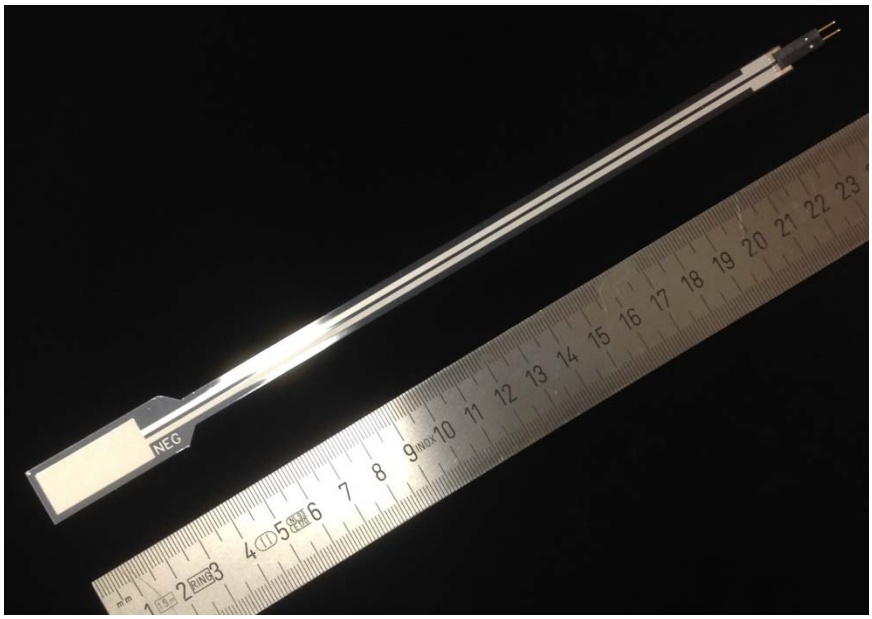

Nominal Capacitance: 1.36 nF
Part Number: 1-1002785-1 Model Description: FDT1-028K [21]

Figure 4. Sensor Type 4

5th Type : Piezo Film with Mylar Protection

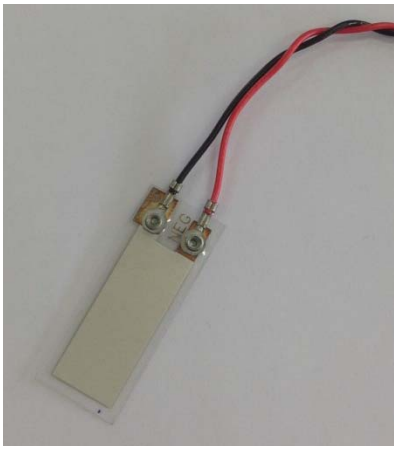

Nominal Capacitance: 1.38 nF
Part Number: 1-1002910-0 Model Description: LDT1-028K [21]

Figure 5. Sensor Type 5

4. Specimen Preparation

The methodology, as well as the procedure of how the PVDF film sensor is placed into a simple composite laminate is extensively described in [21].

For the needs of our study we have extended the manufacturing procedure to include also sandwich composites. Performing the testing campaign on these can be considered as an intermediate level between simple strips and a more complex composite structural performance. Also, the usage and placement of the sensor in sandwich composites is closer to the scope of manufacturing a fully composite container.

In the first instance we selected the metallized silver-ink electrode, unwired, piezo film Type 1 sensor, presented in Figure 1, to be placed within the composite laminate. Dimensions, as well as the properties of the sensor, have been summarized in the previous section. For the fabrication of the sandwich composites, the sensor was placed in the laminate either folded once, or twice, over. The purpose of this folding was motivated by two aspects:

1. The plan area of the sensor was wider than the panel, so it was decided to fold it simply to be able to fit it on the available panel area. The folded sensor width was 65mm, and so it was possible to be placed within a lamination of either 75 or 100mm width as shown in Figure 6.
2. Given that the resulting voltage from the sensor is a function of the average strain generated at the area it covers, the placement of the sensor at the location at maximum strain on the center of the sandwich beam, was therefore expected to provide a higher voltage. This is desirable when embedding sensors for energy- harvesting applications.

4.1 Preparation of Sandwich Composite with Plywood Core

The methodology described in this section refers to the fabrication of the specimens with the plywood core and embedded sensors; however, there are some differences between the types of electrode used. Figure 6 (a) and (b) illustrate the silver-sputtered electrode PVDF sensor fitted with copper-strip terminals (a) placed open plan with copper connectors and (b) folded on top of the plywood core. In this case the area covered by the sensor was 190x65 mm^2. The sensor was placed between the composite skin and the core. The location of the sensor as well as the glass-fiber layers placement prior to the resin infusion is presented in the Figure 7.

For the purposes of this study four different specimens were fabricated with the same type of core. All the specimens are presented in Figure 8 to Figure 11. For specimens 1 to 3 a Type 1 (silver-ink electrode surface) sensor was placed, noting that the sensor in Specimen 3 is placed in the laminate double-folded. In Specimen 4 (Figure 11) we tried out a different technique, a Type 2 metallized PVDF (with Cu Ni electrodes and pre-fitted with connector leads) was bonded directly to the plywood core using an epoxy-

based adhesive film; the scope here was simply to assess the feasibility of bonding the sensor using a heat-assisted pressure cycle up to approximately 60 °, and to examine if it was possible to bond the film directly onto a fibrous surface at temperature without losing the piezo-effect on the PVDF film.

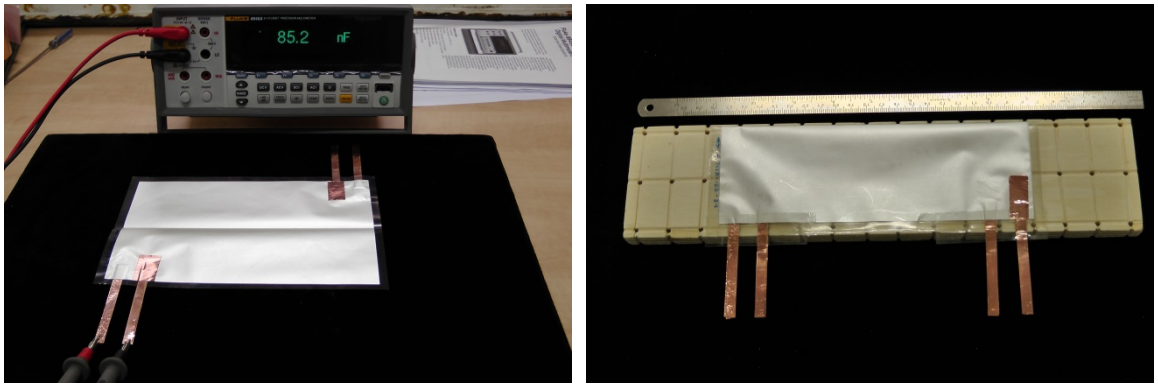

(a) (b)

Figure 6. Metallized Piezopolymer film (a) copper terminal placed on sensor and (b) placement of folded sensor on the plywood core.

Figure 7. Preparation of sandwich specimen prior to resin infusion, with the sensor placed between the core and the composite skin.

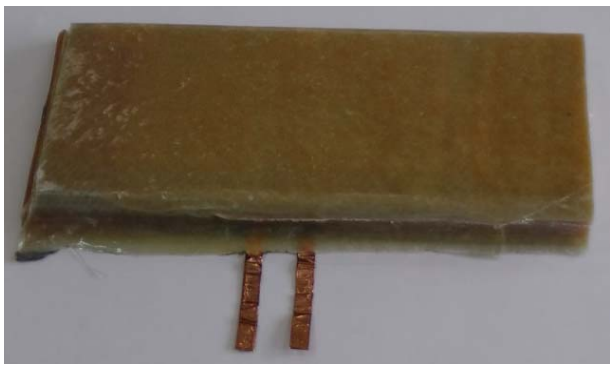

Specimen 1

Sensor Area: *190x62mm^2 folded*

Sensor Type: *Type 1*

Core material : *Plywood*

Electrodes: *Copper*

Dimensions:320x70x22mm^3

Laminaton Configuration: *$[(0/90)_6/Core]_S$*

Figure 8. Plywood core Specimen 1

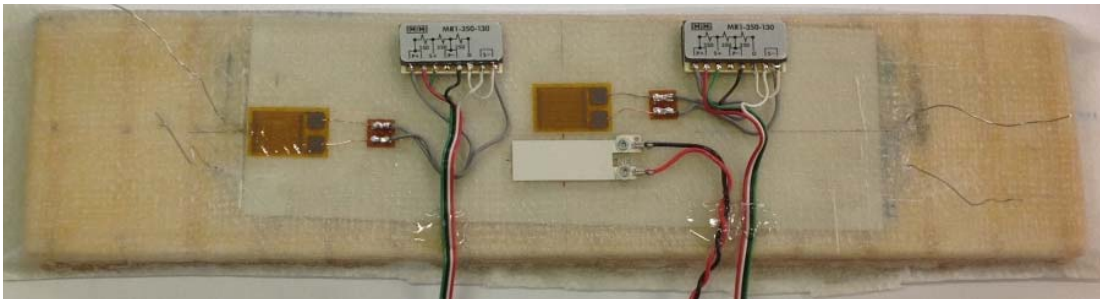

Specimen 2

Sensor Area: *190x62mm^2 folded*

Sensor Type: *Type 1*

Core Material: *Plywood*

Electrodes: *Simple Metallic*

Dimensions: 320x70x19mm^3

Lamination Configuration: *$[(0/90)_6/Core]_S$*

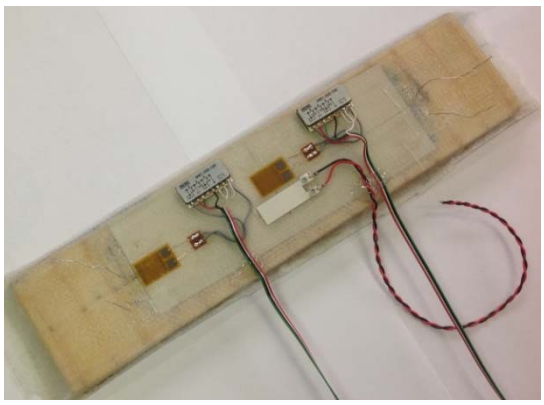

Figure 9. Plywood core Specimen 2

Specimen 3

Sensor area: *95x62mm^2 folded twice*

Sensor Type: *Type 1*

Core Material: *Plywood*

Electrodes: *Simple Metallic*

Dimensions: 320x70x20mm^3

Lamination Configuration: *$[(0/90)_6/Core]_S$*

Figure 10. Plywood core Specimen 3

Specimen 4

Sensor area: *95x62mm^2*

Sensor Type: Type 2

Core Material: *Plywood*

Electrodes: *Simple Metallic*

Dimensions: 320x70x17mm^3

Figure 11. Plywood core Specimen 4

4.2 Foam Core Sandwich Composites

The second group of sandwich specimens tested uses the 3cm thick AIREX T92.90 foam core. Additionally, a slight modification on the ply sequence was used as an additional sub-ply was inserted between the two faces of the folded sensor. This change was expected to improve the quality of the resin infusion between the folded PVDF layers. The steps followed for the specimen preparation are illustrated in Figure 12. Using the methodology described in Figure 12 four different specimens were prepared, two of which had embedded sensors. These are presented in Figure 13 to Figure 15.

Step 1

Folded sensor with cable electrodes

Step 2

Folded sensor placed at the penultimate layer of the composite laminate on top of the foam core. A layer of glass cloth was inserted between the two sides of the folded PVDF sensor.

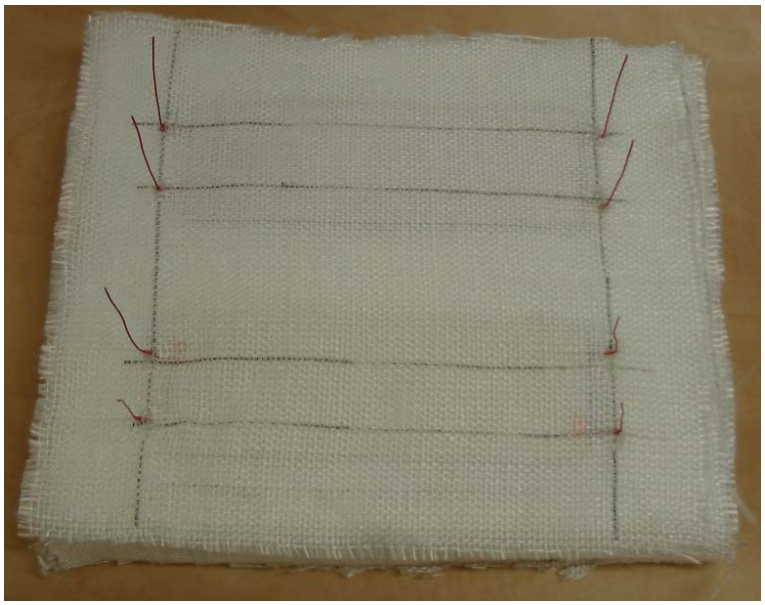

Step 3

A pair of specimens with the embedded sensors placed at the penultimate layer before the resin infusion procedure.

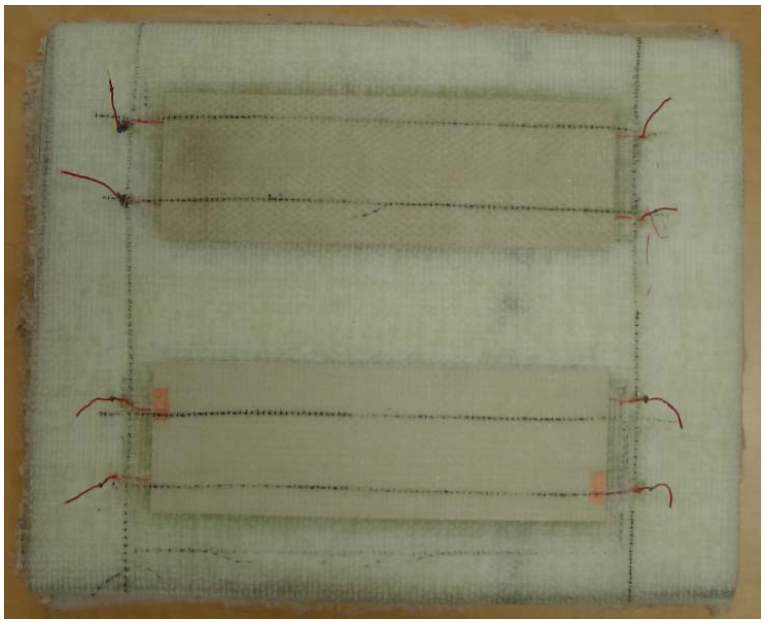

Step 4

A pair of composite specimens with embedded sensors after the resin infusion procedure.

Figure 12. Four steps of the preparation of a pair of foam core sandwich composites.

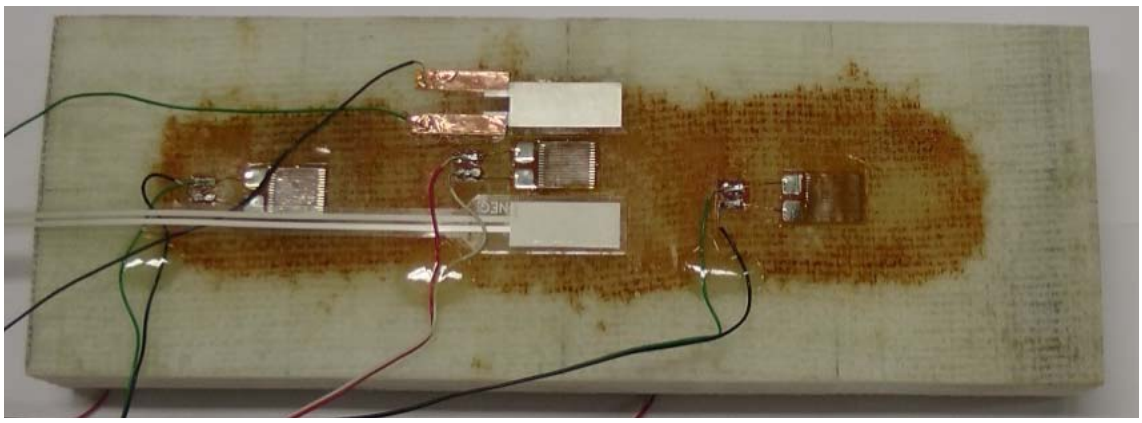

Specimen 5

Sensor Type: *Type 3 and Type 4 (Attached, no Embedded Sensor)*

Core Material: *Airex Foam Core*

Electrodes: *Provided by the sensor or cables*

Dimensions: 280x100x34mm^3

Lamination Configuration: $[(0/90)_8/Core]_S$

Figure 13. Foam core Specimen 5

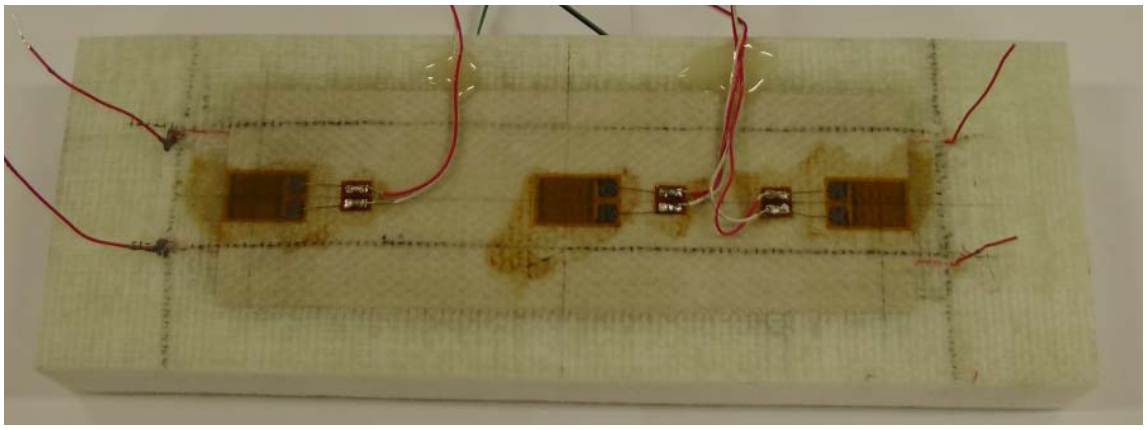

Specimens 6 & 7

Sensor Area: *190x62mm^2 folded*

Sensor Type: *Type 1*

Core Material: *Airex Foam Core*

Electrodes: *Simple Cables*

Dimensions: 280x100x34mm^3

Lamination Configuration: $[(0/90)_8/Core]_S$

Figure 14. Foam Core Specimens 6 & 7 (image above illustrates only specimen 6).

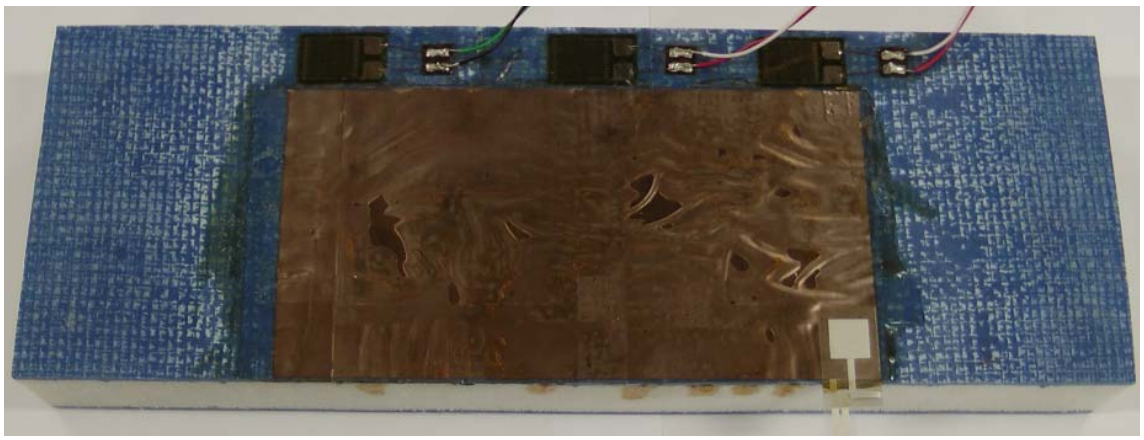

Specimen 8

Sensor Area: *95x62mm^2 attached on the surface*

Sensor Type: *Type 2*

Core Material: *Airex Foam Core*

Electrodes: Provided by the sensor

Dimensions: 280x100x34mm^3

Lamination Configuration: *$[(0/90)_8/Core]_S$*

Figure 15. Foam core Specimen 8

5. Instrumentation and experimental set-up

As well as gaining a heuristic insight into the manufacture of sensor-embedded composite panels, another objective of the current study is to investigate the quasi-static and fatigue performance of the manufactured elements. The experimental campaign involves cyclic testing of sandwich specimens with and without intra-laminar embedded sensors subjected to 3-point bending loading. An MTS testing frame was used with a capacity of 50KN (Figure 16). The actuation signals were generated via a Labview VI application, the signal was then digitized using a National Instruments, NI 6229 board and finally driven to the terminals of the MTS controller.

To measure the system response and calibrate the PVDF sensors, strain gauges were placed on the specimen surface as close as possible to the attached piezopolymer sensors. Both types of signal were acquired and digitized via the appropriate signal conditioning boards of a SCXI chassis. The strain gauges we used had resistance of 350 Ohms, suitable for polymer matrix composite materials, avoiding generation of excessive local heating, operating under a full or quarter bridge configuration. Additionally, the applied displacement from the stroke on the three point bending tool as well as the resulting force on the specimen were recorded. The digitized signals

were all further analyzed and plotted as a function of the number of loading cycles performed on the testing frame.

5.1 Dynamic Performance

All the specimens were tested under three-point bending configuration with cyclic sinusoidal loading. The purpose of using a dynamic setup was based on the basic working principle of using piezoelectric devices (which are also electrical capacitors), and for which the application of a dynamic load generates a charge between the two electrodes on either side of the PVDF film. The sensor when loaded with a parallel resistance acts as an electrical resonator having a -3dB cut –off frequency given by $fc=1/2\pi RC$, where R is the resistive load and C is the capacitance of the device .The effect of this dynamic cut-off frequency is such that at static and low frequencies well below fc, the output generated by the device will be proportional to the rate of change of strain (hence very low electromechanical transduction), whereas for excitations above fc, the output will be constant for a given strain amplitude; i.e., a dynamic self-excited strain gauge.

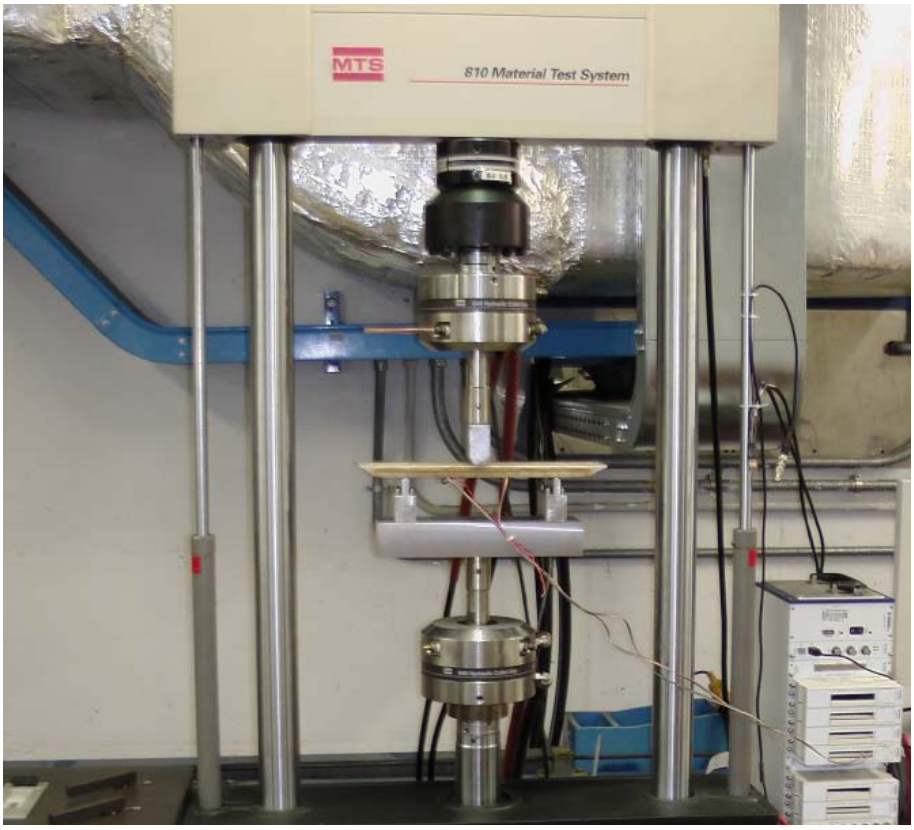

Figure 16. 50KN capacity testing frame.

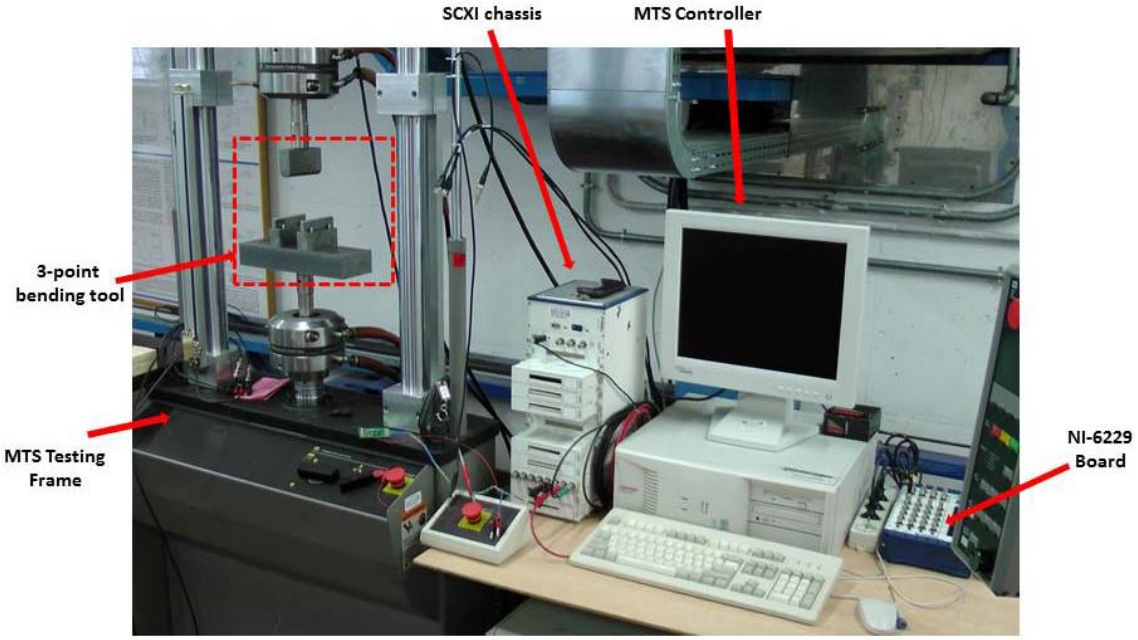

Figure 17. Experimental setup for quasistatic testing.

To conduct the tests a three-point bending set up was selected (in order to introduce both tensile and compressive stresses), as this simulates a more realistic loading condition for a composite structure during service life. The experimental setup used is illustrated in Figure 17. The actuation consists of a sinusoidal signal in the range between 1 to 10 Hz under displacement control. As described earlier, the signal generated on Labview, was used to drive the MTS controller from the analogue output of an NI-6229 board. For each test there was synchronous acquisition of the voltage from each PVDF sensor as well as the applied displacement and the resultant force from the specimen using an SCXI-1140 module. Simultaneously, the strains recorded from the strain gauges adjacent to the sensors were continuously recorded from an SCXI-1520 strain gauge conditioning module (both full and quarter bridge voltages were used without significant discrepancy in the results). In order to eliminate the effect of the static strain offset, the sensitivity of each of the sensors was extracted as the ratio of covariance of the generated strain over that of the resultant voltage from the sensors.

6. Results and Discussion

The key experimental aspects reported below concern the effects on the sensitivity of the rate of loading, the amplitude of excitation and the sensitivity of the devices to embedding and bonding interfaces. The results do not purport to validate the quality of the specific brand of PVDF products but rather their generic behavior.

6.1 Plywood Core Specimen

6.1.1 Tested specimen and setup

The tested specimen is shown in more detail in Figure 18 illustrating the extension of the embedded folded PVDF area, the two surface-mounted patch sensors and the standard strain gauges. It has been mentioned in Section 3 that plywood was used as a core material simply for expediency in order to observe the effectiveness and survival capacity of embedding a sensor during sandwich panel production. Surprisingly, not only did the procedure appear to be successful (the electrical connectivity of the embedded sensor was assured), but it was apparent that the structural properties of component, as will be shown below, were satisfactory.

6.1.2 Measurements

Various frequency levels were selected for the applied actuation signal. Figure 19 (a) to (d) illustrate typical applied displacement and the resultant signals for force, strain and sensor voltage respectively. The measured strains on the two gauges, placed on the middle and at the edge of the embedded sensor area are presented in Figure 20 (a) and (b) respectively.

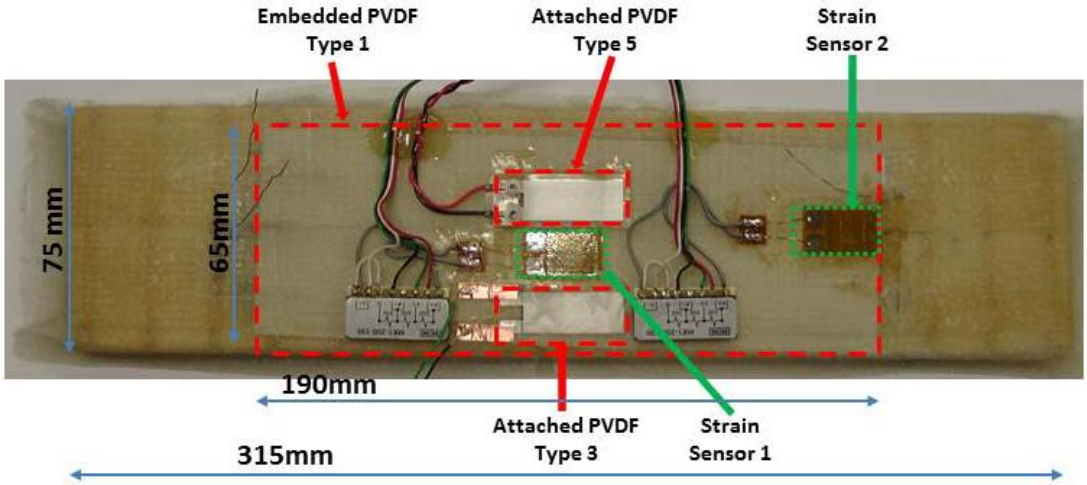

Figure 18. Location and type of the PVDF and strain sensors placed through the thickness and at the surface of the tested sandwich specimen.

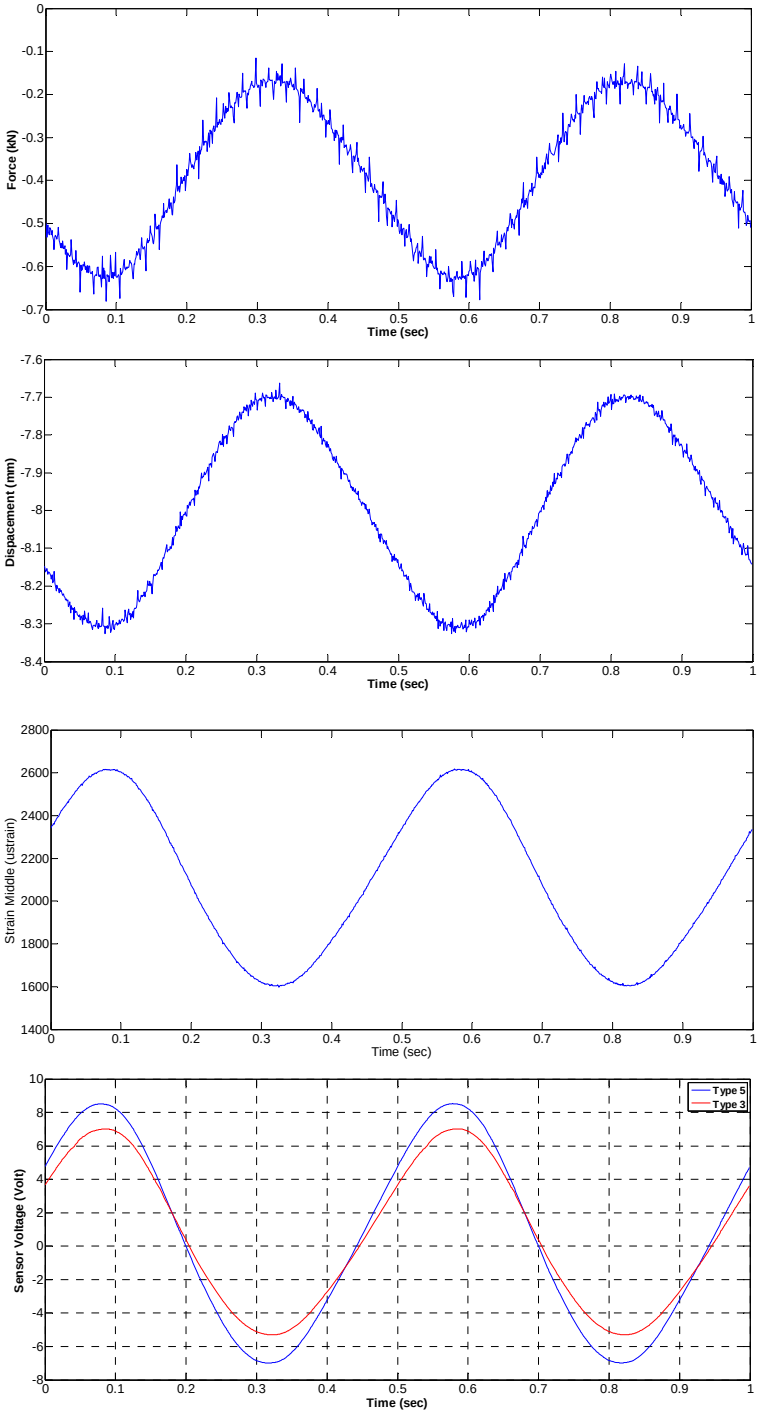

Figure 19. Experiment at 2Hz, (a) applied displacement and (b) reacting force from the specimen.

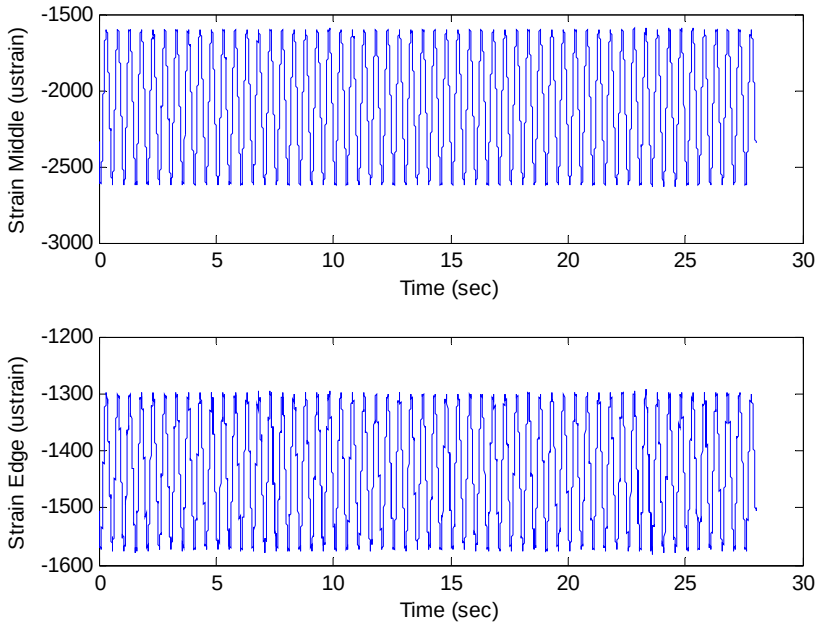

Figure 20. Representative generated strain time series of the two strain gauges located (a) at the middle and (b) over the edge of the embedded PVDF sensor.

The measured voltages from each of the three piezopolymer sensors are illustrated in Figure 21 (a) to (c) as a function of the average generated strain at the middle of the composite beam span. The sensitivity[2] of each sensor is indicated on top of each graph. There are some important conclusions to be made from these plots:

a) The sensitivity measured from the small piezopolymer, Type 5 approximates to the theoretically estimated range (41-82 μstrain/Volt) based on the manufacturer's declared specific properties and dimensions of the sensors
b) The sensitivity of the sensor Type 3 is about 25% lower compared to the theoretical estimation (i.e., more strain is required for the same voltage generation). Possible reasons for the reduction to the sensitivity include (i) the placement of the sensor eccentrically relative to the specimen width, as illustrated in Figure 18, located at the edge of the specimen and (ii) the theoretical value of the sensitivity is highly dependent on the Young's modulus ranging from 2-4 GPa. The sensitivity of the large embedded sensor was measured to be about 126 μstrain/Volt, which is about half of the expected value assuming that the theoretical estimation for this thickness was to be the same as for the sensors Type 3 and 5. We arrived at this value by estimating the weighted average strain over the area covered by the embedded metallized piezo film. This disagreement arises probably due to the variation of the strain field through the thickness of the sandwich composite laminate. The placement

[2] Sensitivity could be defined as the voltage produced for a given strain. However, we represent the sensitivity in ε/Volt, thus a 10 ε/Volt sensor is more strain sensitive than a 100 ε/Volt sensor.

of a piezopolymer sensor at the penultimate layer of the top face of the composite skin, especially in a folded configuration results in a complex strain distribution on the sensor faces. Clearly, the interpretation of strain field of a folded film depends on the assumption that the interface between the matching faces is perfect. In order to monitor this interface it will be necessary to cut a section through the specimen and examine it under an optical microscope.

c) The voltage versus strain curve provided by the sensor Type 3, Figure 21 (b), approximates to a straight line, indicating that there are no major hysteretic phenomena for this sensor. On the other hand the same curve for small patch-sensor Type 5, Figure 21 (c), reveals a hysteresis loop. The most probable reason of this hysteretic behaviour is the presence of a thick (88.5 μm) protective layer of *Mylar* (*Molten Polyethylene Terephthalate: PET*) on each side of the sensor. We conjecture that the hysteresis arises because of the viscoelastic properties of this material.

d) Concerning the energy transduction efficiency, (which is the main function we propose for using this type of sensor geometry), the recorded voltage, as expected, is higher for the sensor with the higher sensitivity. However, a combination of a sensor with high capacitance and sensitivity can potentially operate as an energy harvesting device.

6.1.3 Parametric sensitivity analysis: strain amplitude and frequency

The parameters that affect the measured sensitivity of a sensor were further investigated. In Figure 22 (a) and (b) we present the variation of the measured sensitivity as a function of the frequency of actuation.

These measurements indicate that there is a slight reduction of the sensitivity recorded for the PVDF Type 5 as the frequency increases, whereas the sensitivity of PVDF Type 3 remains insensitive to the frequency changes. This observation is probably due to the hysteretic phenomena of the Mylar layer, given that the viscoelastic behavior of a structure is strongly related to the oscillation frequency. On the other hand, the behavior of the large embedded sensor indicates small variations. These discrepancies become more acceptable assuming that this sensor response was related to the strain generated in a bigger area (almost half of the specimen total area).

The effect of varying the amplitude and, as a consequence, the level of developed strain was further investigated. For this study two different frequency levels were selected for the applied load on the specimen, specifically at 5 and 10 Hz. During the testing procedure the specimen was preloaded to 0.36KN for both frequency cases. Measurements of the sensitivity as a function of the average strain deviation on the composite structure during loading are presented in Figure 23 and Figure 24. All the sensors presented a similar sensitivity trend, i.e. remaining insensitive (or with a slight increase) as the strain on the structure increased. This observation is important if the device were to be used as a linear strain gauge.

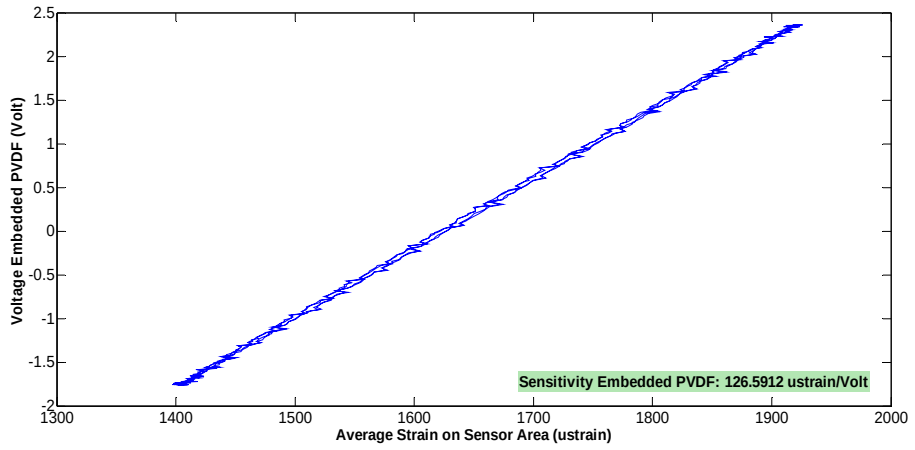

(a)

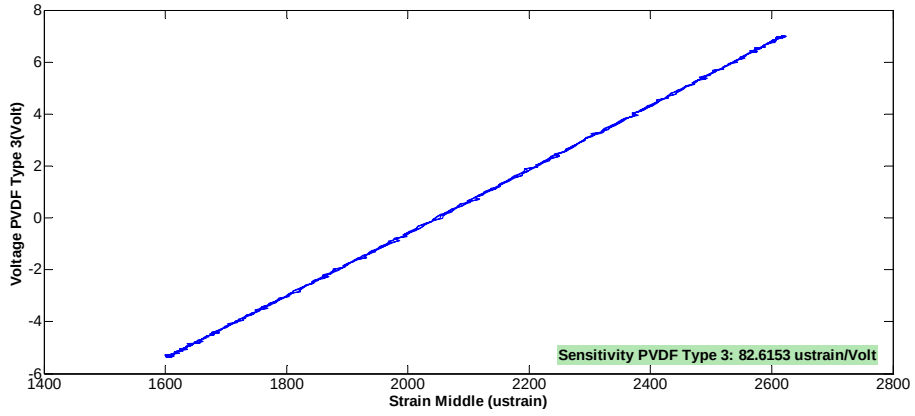

(b)

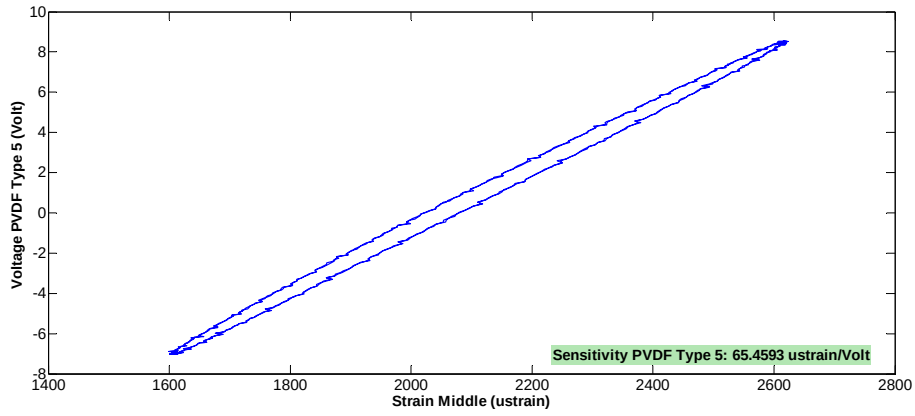

(c)

Figure 21. Variation of the measured sensor voltage as a function of the generated strain, (a) above the embedded PVDF Type 1, or (b) next to PVDF Type 3 and (c) next to PVDF Type 5.

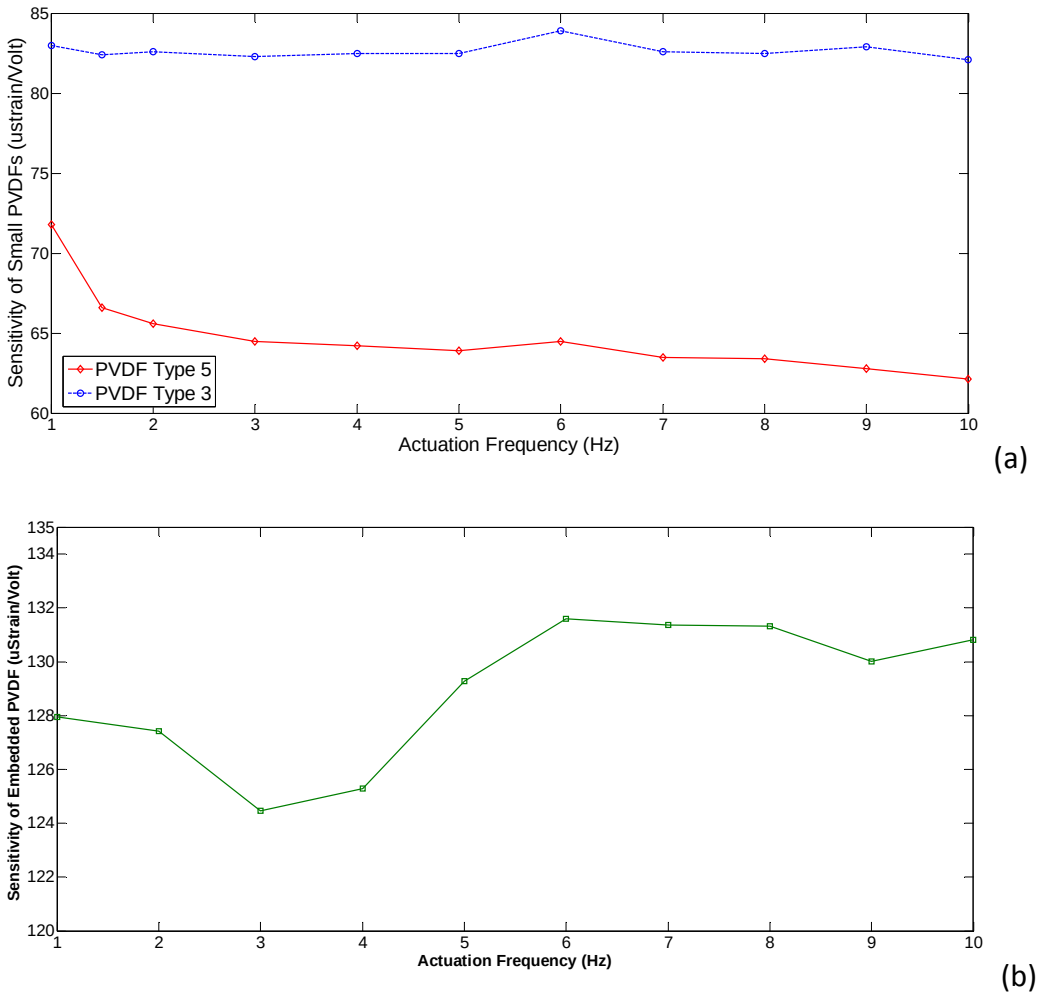

Figure 22. Piezopolymers sensitivity as a function of the actuation frequency (a) PVDFs Type 3 and 5 and (b) Embedded PVDF Type 1.

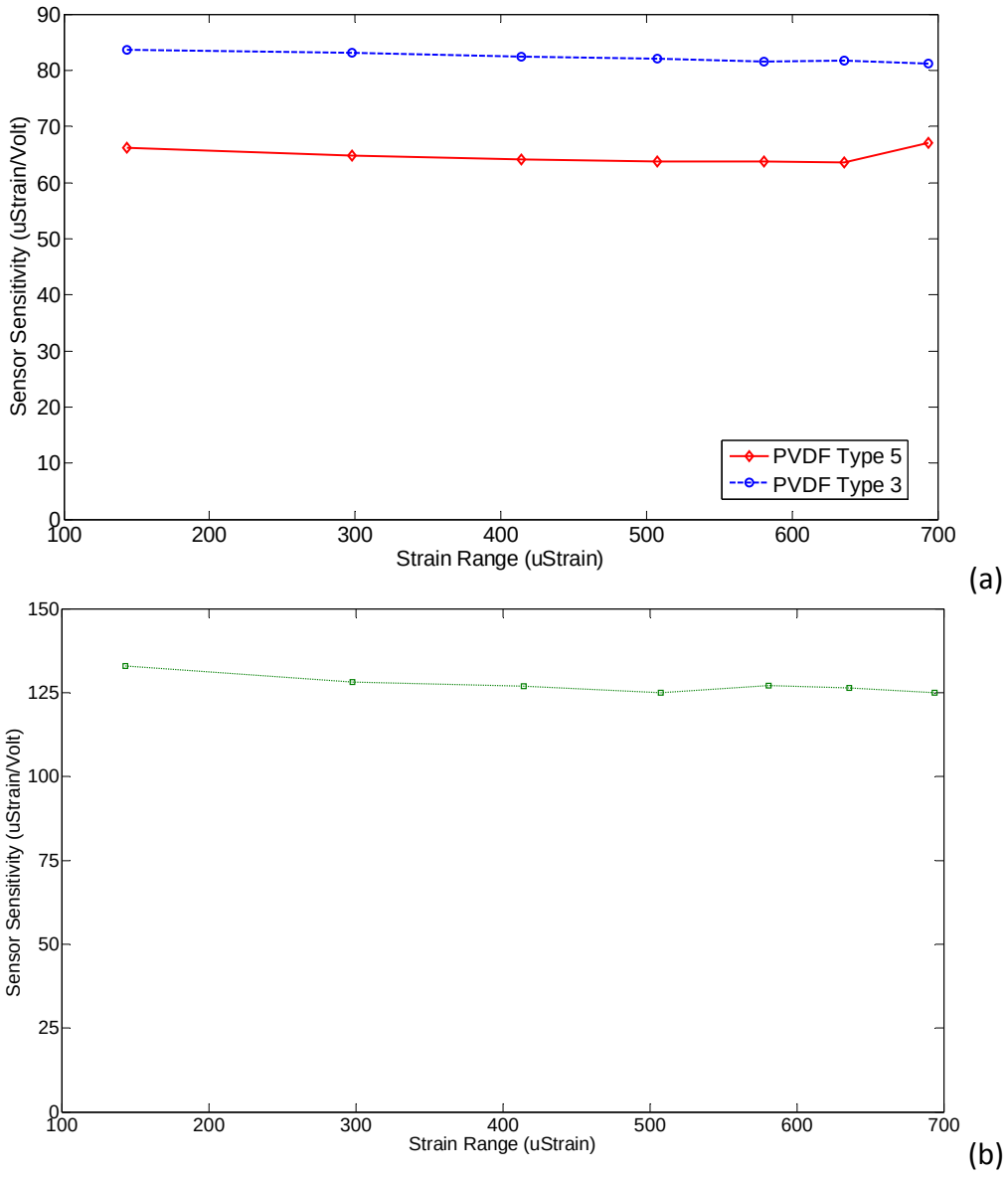

Figure 23. Piezopolymer sensor sensitivity as a function of the resulting force on the specimen for actuation at 5Hz, (a) PVDFs Type 5 and 3 and (b) embedded PVDF Type 1.

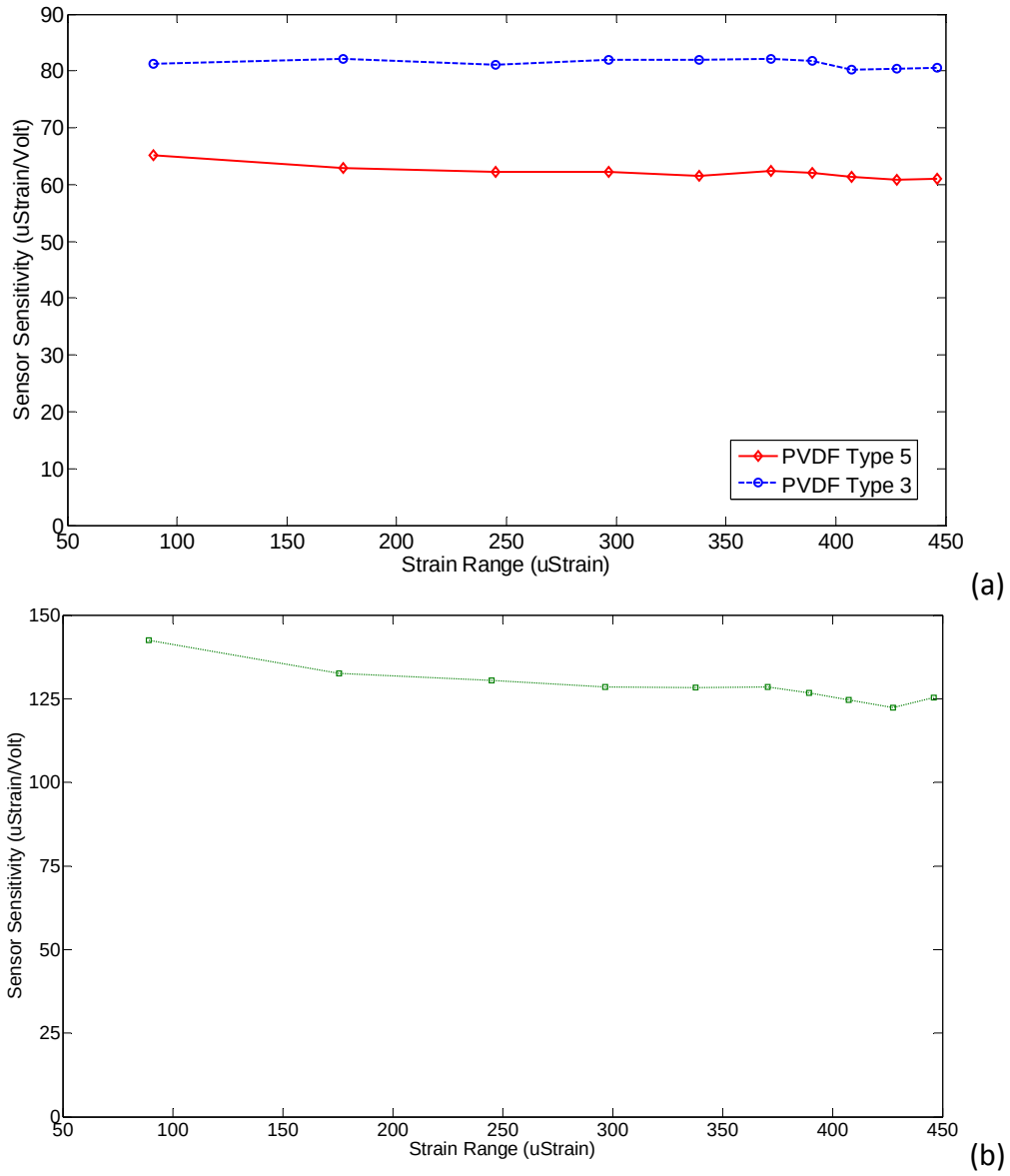

Figure 24. Piezopolymer sensor sensitivity as a function of the resulting force on the specimen for actuation at 10Hz, (a) PVDFs Type 5 and 3 and (b) embedded PVDF Type 1.

6.2 Foam Core Specimens

6.2.1 Testing of superficially mounted sensor

A sandwich panel manufactured using a synthetic core material, Specimen 8, was tested having a Type 2 (Cu-Ni electrode) piezopolymer sensor attached on the surface. Additionally, three strain gauges were placed next to the sensor for calibration purposes as shown in Figure 25.

In order to provide a more realistic estimation of the generated strain across the skin of the sensor, the weighted average measured strain along the length of the sensor patch was calculated. The measured sensor voltage, as a function of the generated strain during the vibration at 3Hz is presented in Figure 26. From the measurements it appears that there are no noticeable hysteretic phenomena recorded, reinforcing the conclusion that when there is no protection coating on the sensor the phase delay between the generated voltage and the periodic loading is almost negligible.

The sensor sensitivity was measured at approximately 49μstrain/ volt, whereas the expected sensitivity for this thickness of sensor (56μm) is 33 μstrain/ volt [21]. This discrepancy falls within the range attributable factors, including; imprecise knowledge of the PVDF Young's modulus (and other physical parameters such as permittivity and electromechanical conversion factors) as well as imperfections of the bonding surface area. The variation of the measured sensitivity was studied as a function of the frequency of the period of excitation. The applied displacement was calibrated in order to monitor the result for the same strain variation in all the frequency ranges, which was approximately 250μStrain.

Figure 25. Specimen 8, foam core sandwich composite with attached a Type 2PVDF sensor.

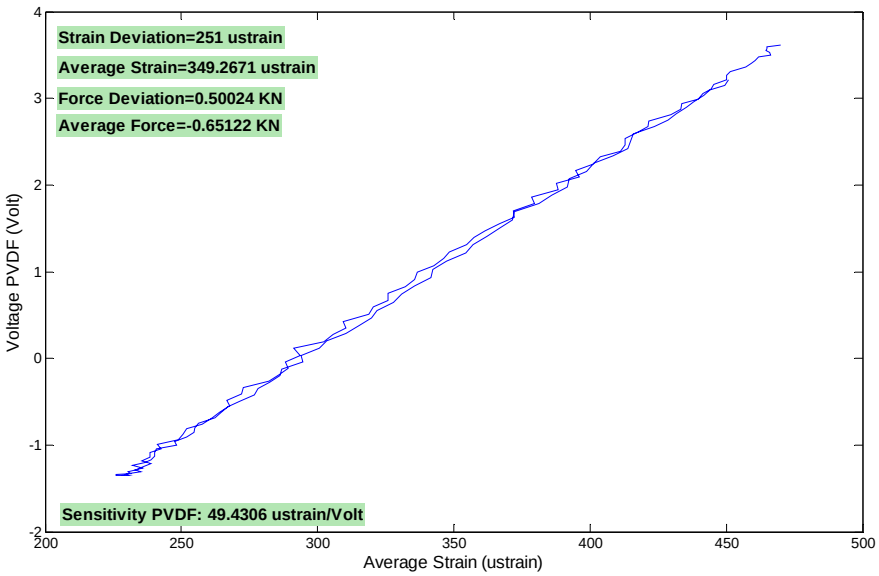

Figure 26. Variation of Sensor Voltage as a Function of the generated strain on the skin.

Figure 27 (a) presents an almost constant variation of the sensitivity as a function of the applied actuation frequency. This indicates that the capability of the sensor to generate voltage on the terminals remains constant irrespective of the applied frequency. For validation purposes the deviation of the average developed strain on the surface for each frequency level is indicated in Figure 27 (b).

Additional experiments addressed the variation of the sensitivity as a function of the applied displacement on the specimen for two frequency levels, 5 and 10 Hz. Measurements are illustrated in Figure 28 (a) and (b) for 5 and 10 Hz actuation respectively. The 1st plot illustrates a slight variation on the measured sensitivity indicating that the ability of the sensor to generate voltage is almost constant and insensitive to the applied load. On the other hand discrepancies were recorded on the sensitivity variation as a function of the increased load for the case where the actuation was set at 10Hz. The performance of the sensor to generate voltage as a function of the increased applied load is illustrated in Figure 29 (a) and (b).

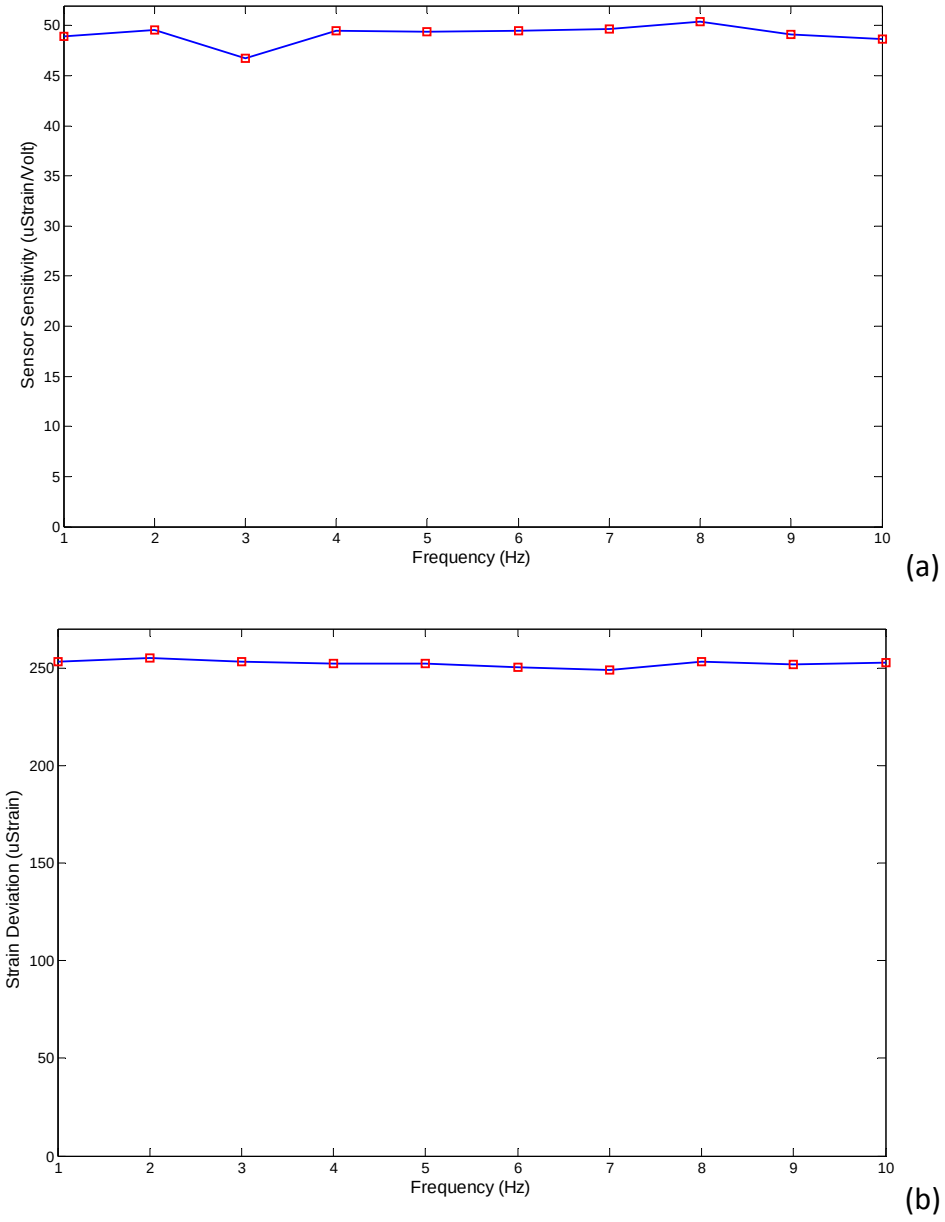

Figure 27. Frequency dependent variation of (a) sensitivity and (b) the generated strain.

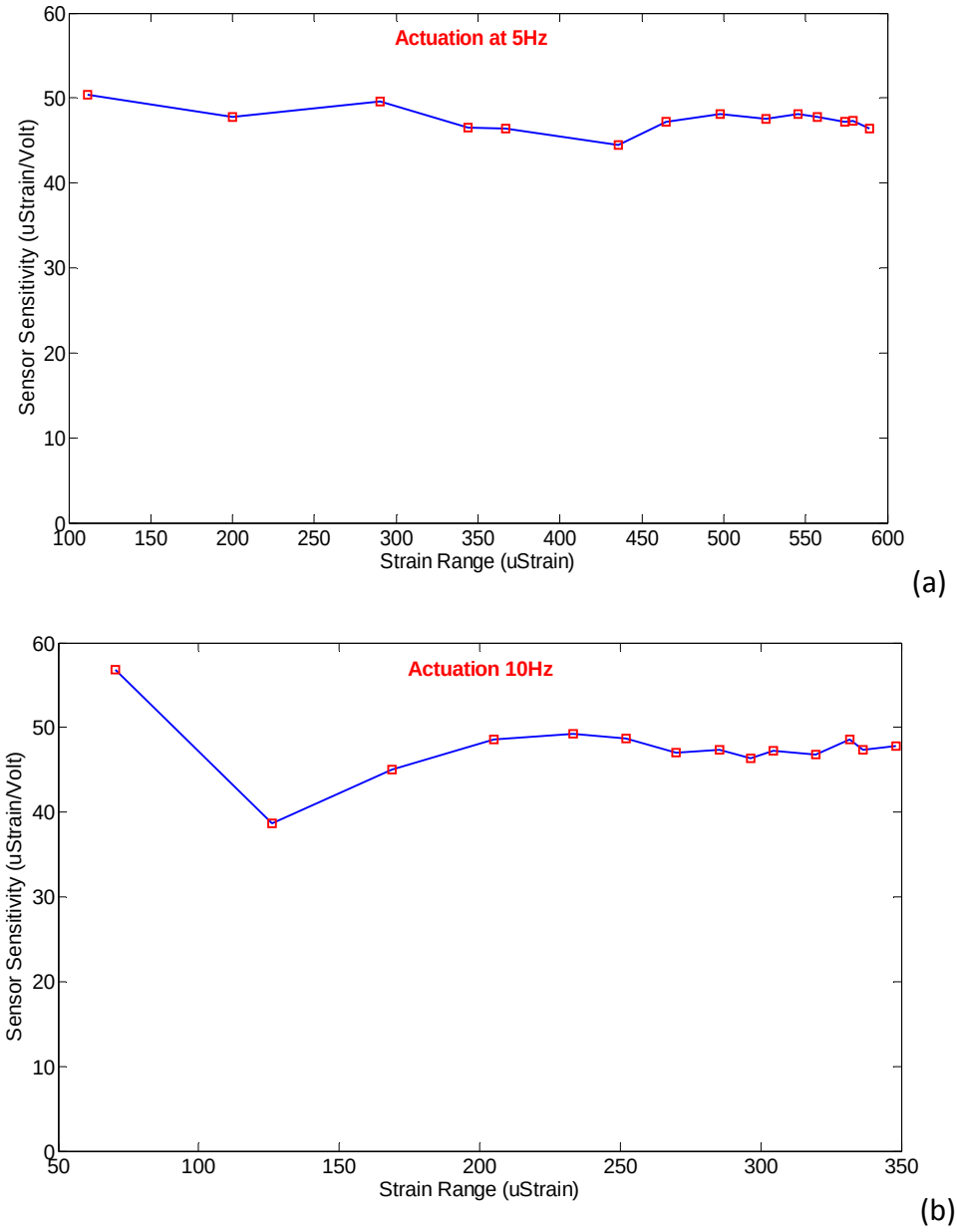

Figure 28. Variation of Sensor Sensitivity as a function of the generated strain when periodic actuation was set (a) at 5Hz and (b) at 10Hz.

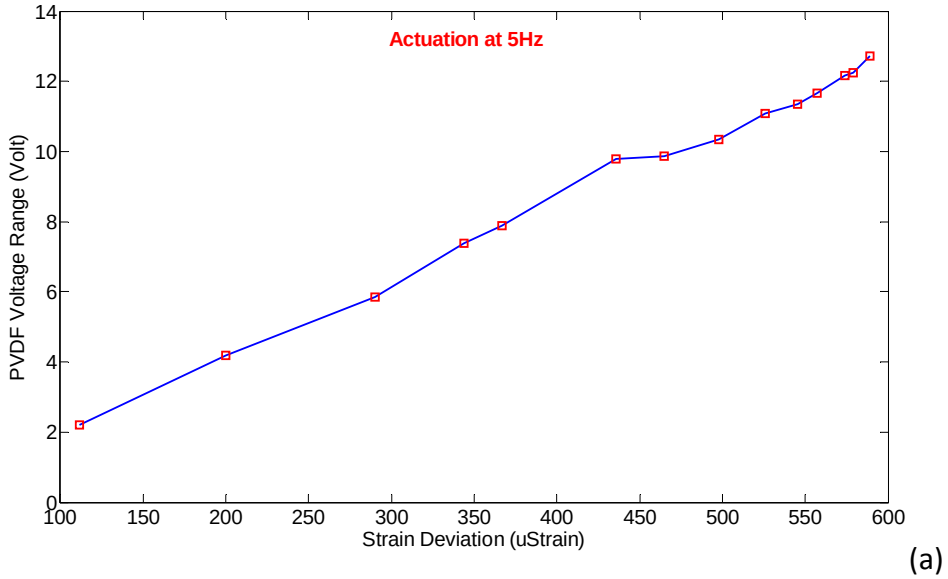

(a)

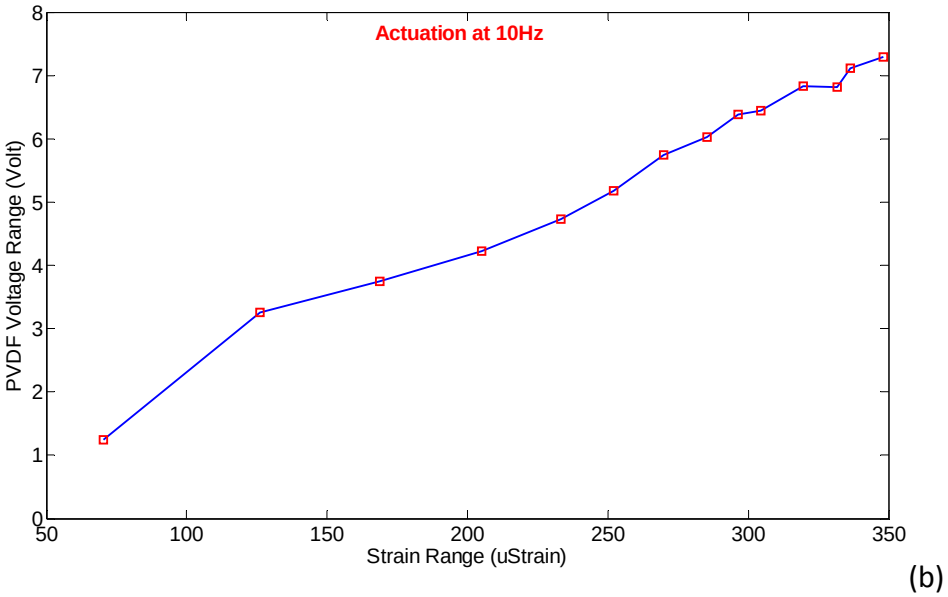

(b)

Figure 29. Generated voltage at the terminals of the attached PVDF as a function of the average developed strain, (a) actuation at 5Hz and (b) actuation at 10Hz.

6.2.2 Sandwich specimens with embedded PVDF sensors

This section describes the testing of a pair of foam core specimens fabricated in a single batch with the procedure presented in section 4.2. These are Specimens 6 and 7 as shown in Figure 14, containing a folded Type 1 metalized piezofilm. The objective of the study was the investigation of the specimens' performance and the repeatability of the fabrication procedure. This pair of specimens had only small variations in their nominal composite skin thickness; indicating a good quality of the resin infusion process. However, there was a minor difference in the specimens in so far as the location of one of the sheet sensors was shifted by 2mm with respect to the center line. Otherwise, the sensor type and dimensions were acceptably equal.

Each specimen was equipped with three strain gauges attached on the surface above the embedded sensor. The position of the PVDF and the strain gauges, as well as the specimen dimensions, is presented in Figure 30. Figure 31 (a) and (b) present the variation of the generated voltage on the terminals of the embedded piezopolymer sensor as a function of the average measured strain across the length of the skin when the specimens are excited at 1Hz. Both of the specimens were subjected approximately to the same strain deviation and the first observation is that neither illustrates significant hysteretic behavior. However, as was the case for the folded specimens using the plywood core, both specimens present a lower than expected sensitivity, varying between 150 and 175 μstrain/volt, whereas for this thickness of sensor the expected sensitivity should be in the range 41 to 82 μstrain/volt. Possible reasons for this discrepancy are concentrated on the methodology followed during the fabrication procedure, which entailed positioning of the folded sensor and the insertion of a ply of glass fibre cloth between the folds.

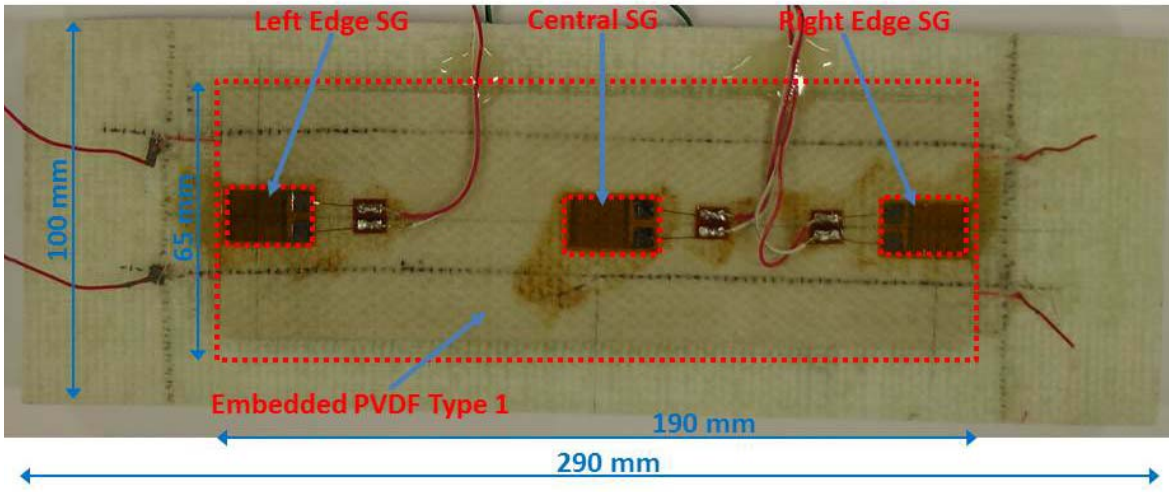

Figure 30. Foam core specimens with embedded metallized piezo film.

Again, this complex geometry is expected to create a significantly complex strain field through the thickness of the sensor and, especially, at the sensor interfaces, which will vary significantly from that developed on the specimen surface and that expected from the theoretical calculation. The purpose of placing the ply of cloth between the two sides of the folded sensor was to achieve a uniform infusion of the resin between the fold. In order to identify if this objective was achieved, a section and microscopic examination through the specimen will be required after the further testing on these specimens has been concluded.

Concerning the recorded difference between the two specimens' sensitivity, this is probably due to the slight misalignment of the sensor location across the length of the ply (we could not ensure that during the vacuum resin infusion the layers may have shifted slightly from their nominal central position). Nevertheless, considering the multitude of inherent physical parameters that affect sensitivity, as well as geometric aspects including asymmetry in the loading configuration, the repeatability of the sensitivity (for not quite identical specimens and manufacture) is, at this stage, acceptable.

The variation of the sensitivity was also studied as a function of the frequency of the sinusoidal actuation and the measurements for both specimens are illustrated in Figure 32 (a). During this experimental study the applied displacement was calibrated to generate a strain deviation during oscillation of approximately 300μstrain (Figure 32 (b)). Both specimens present a similar trend, indicating the ability of the sensor to generate approximately the same voltage on its terminals, irrespective of the frequency (above 1Hz) of the applied force of the specimen. The last part of the experimental investigation concerned the sensitivity as a function of the mean applied displacement. Measurements are illustrated in Figure 33 (a) and (b) for the actuation signal set at 5 and 10 Hz respectively. Both specimens illustrate similar behavior, indicating a slight decrease of the sensitivity as the applied load was increased, especially when the actuation was set at 10Hz.

Summarizing, the results from this pair of, nominally identical, sandwich composites with embedded sensors, indicate that apart from slight differences of the measured sensitivity, both specimens presented similar trends as a function of the applied frequency and force.

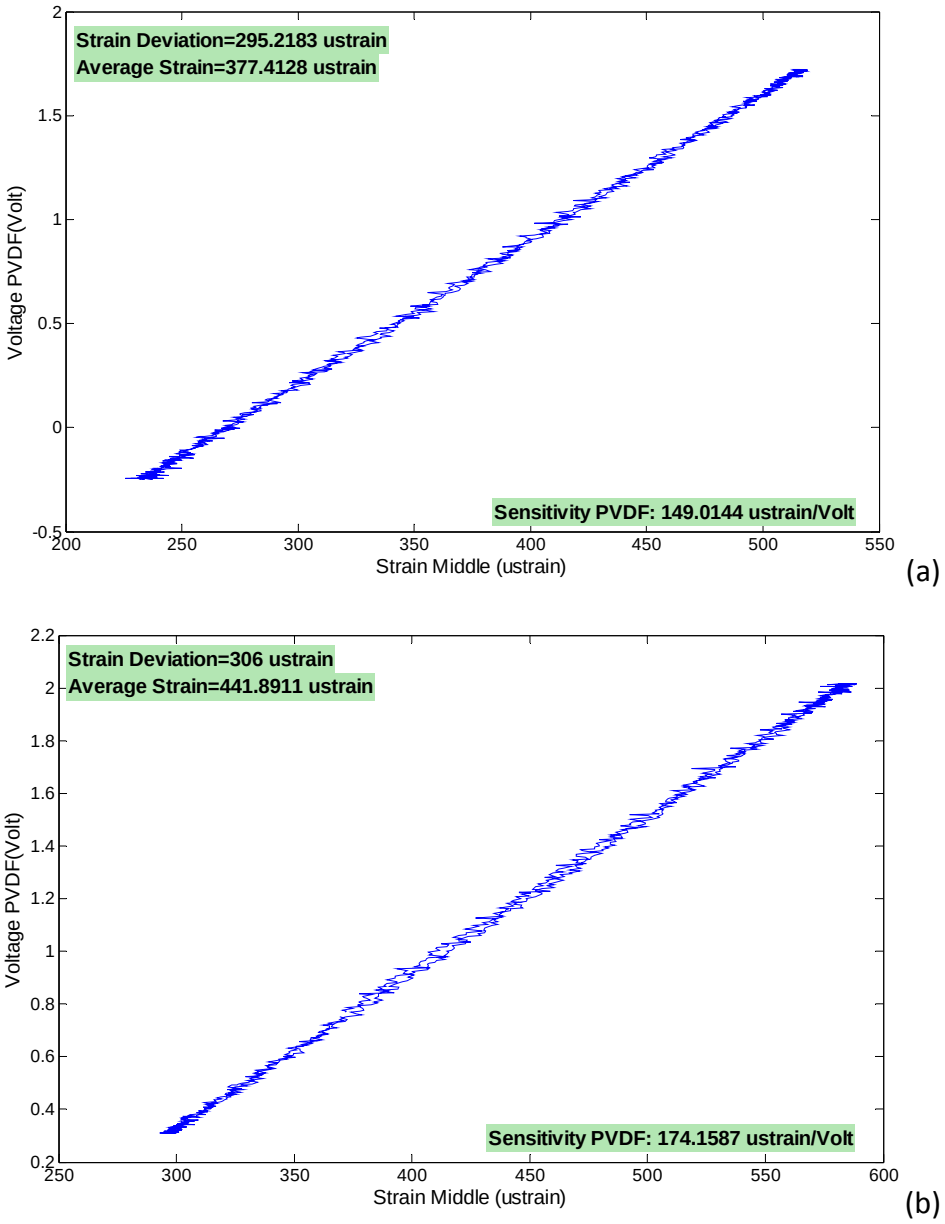

Figure 31. Sensor Voltage versus the average resulting strain (a) Specimen 1 and (b) Specimen 2.

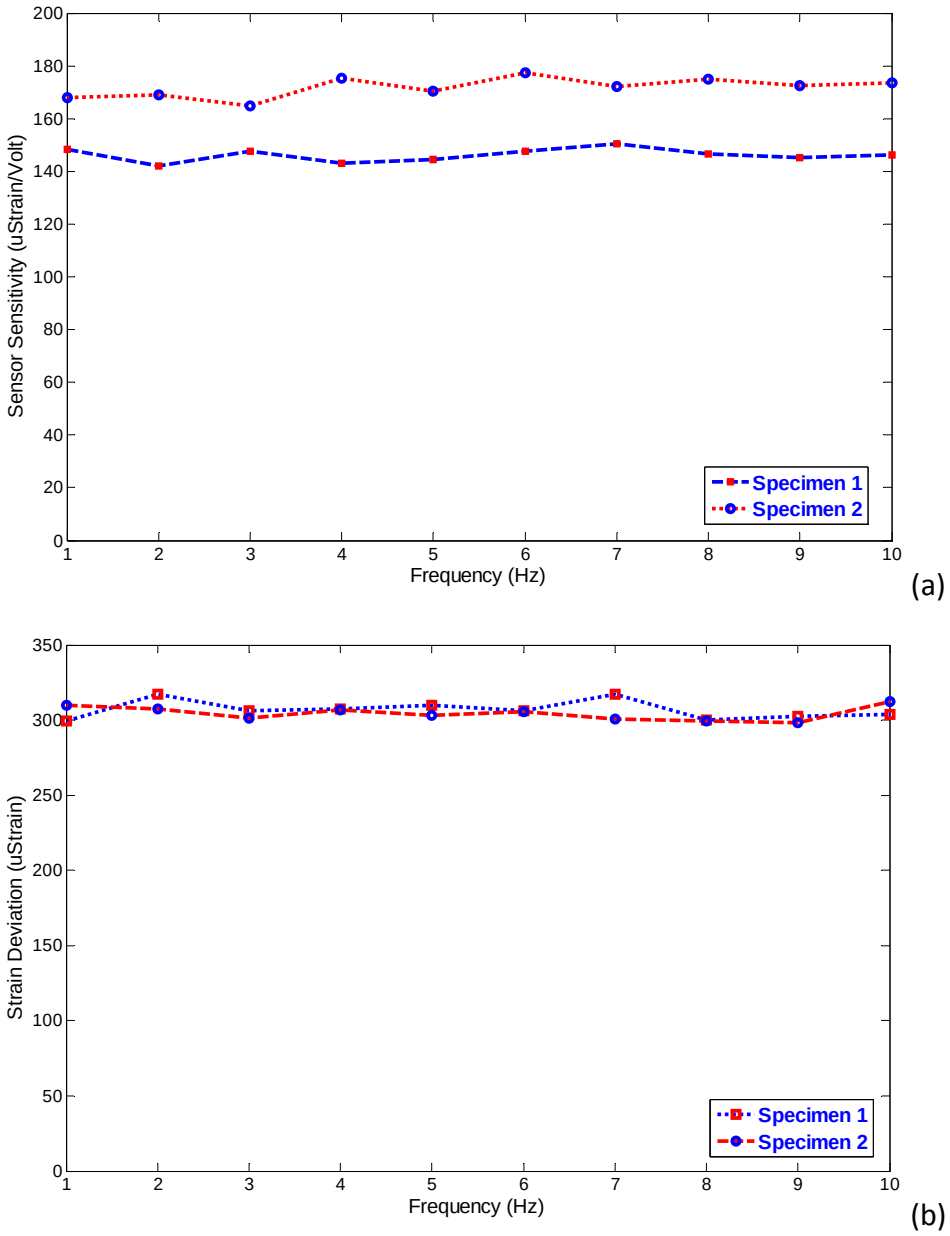

Figure 32. (a) Sensitivity of embedded PVDF versus the applied frequency and (b) developed strain deviation for each of the frequency levels.

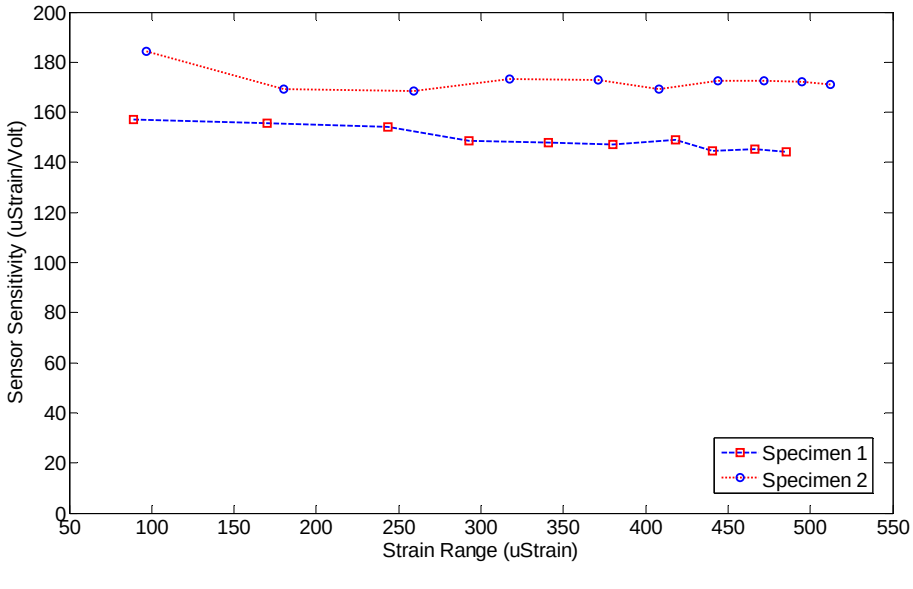

(a)

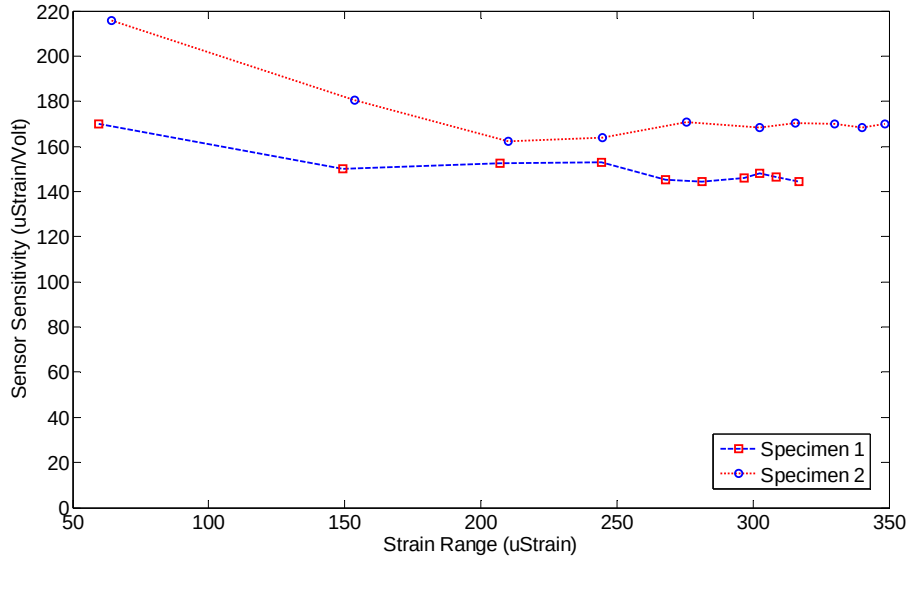

(b)

Figure 33. Embedded PVDF sensitivity as a function of the developed strain deviation on the sandwich skin when actuation was applied (a) at 5Hz and (b) 10Hz.

6.3 Visual Inspection of Embedded Sensor Cross-Section Bonding Interface.

As was stated at the start of this report, one of the aims of these tests was to try out sensor-embedding techniques using direct vacuum-assisted resin infusion. It was clear from the outset that the effectiveness of the method would depend on (i) the flow of the resin through the various lamination layers and, (ii) the interface between the sensor electrode surfaces and the reinforcement layers.

It was decided to examine this problem by cutting a section through the thickness of simple laminates and the plywood sandwich panel fitted with two types of sensor surfaces. For the case of the plywood laminate it became clear that if insufficient flow is achieved between the layers, a delamination layer develops through the thickness of the composite laminate which one must assume will affect the composite's functionality; both mechanical and electrically. Initially, the plywood sandwich panel, Specimen 1, was cut revealing that the two faces of the sensor were completely separated with no sign of resin between them (the perimeter fold had been purposely sealed leaving a resin-dry pocket). Figure 34 (a) and (b) illustrate the sections of the Specimen 1 after cutting, showing a clear separation between the surfaces. However, as illustrated in Figure 35 the bonding between the sensor with the silver-ink coating and the epoxy resin to the laminate layers on either side of the fold appeared to be sound (so that it is impossible to remove the sensor from the composite ply without splitting it). This confirms the potential to embed a piezopolymer successfully within the thickness of a composite laminate; but setting the sensor in the folded configuration requires further investigation at the adhesion to be improved.

Upon examination of a composite plate fitted with an embedded sensor using Cu-Ni electrode surfaces, (Type 2) it became apparent that this electrode material may not always be compatible with the current epoxy resin infusion matrix system. Figure 36 presents the complete de-bonding between this type of sensor and the composite laminate. However, as was shown in the case of Specimen 8, when the resin is applied on the dry finished laminate, the bonding effectiveness is particularly good. These aspects and how they affect bonding at the interface and the resulting strain transfer to the PVDF layer are still to be satisfactorily explained; but certainly proper care in preparing the electrode surfaces prior to infusion is required in order to obtain a good bonding interface. Further corroboration using a more statistically significant number of examples needs to be conducted.

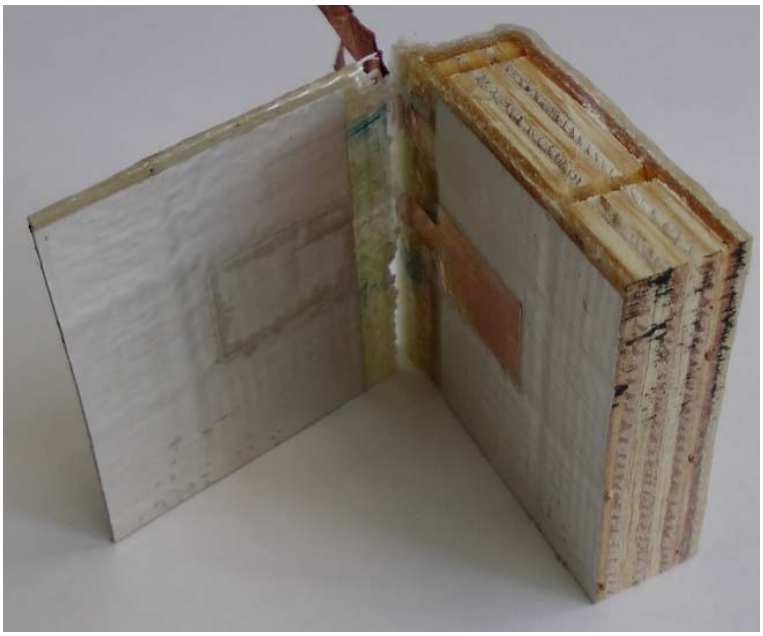

(a)

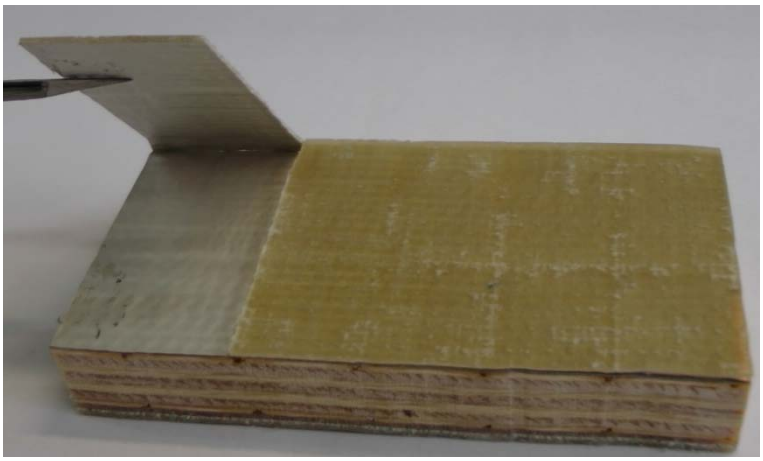

(b)

Figure 34. Lack of resin at the area between the two sides of the folded sensor.

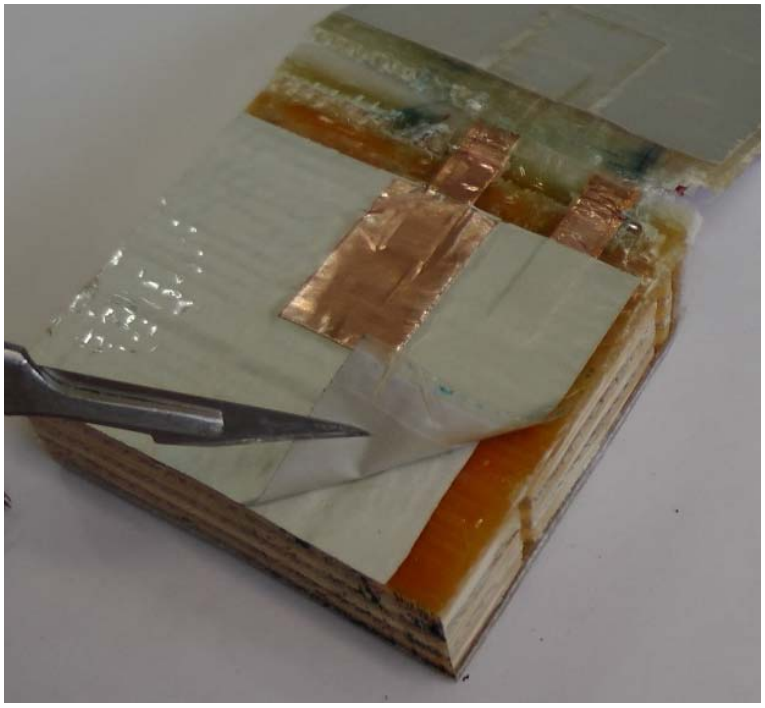

Figure 35. Detail showing where lower fold is still bonded to the composite laminate.

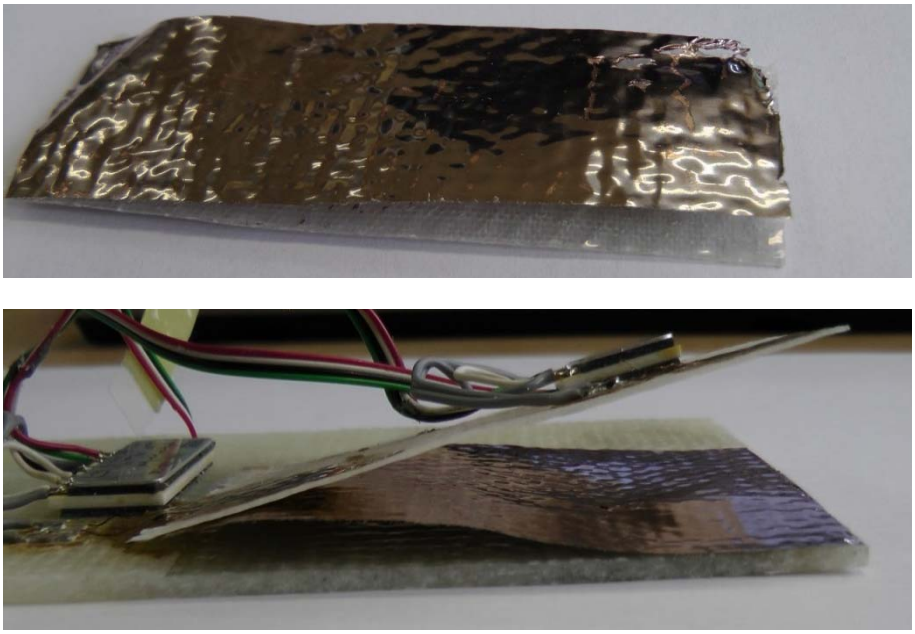

Figure 36. Incompatibility between the composite laminate and the copper coating PVDF sensor.

7. Conclusions

In this report we present the basic principles of our investigations for embedding sensors and energy-harvesting devices in sandwich composite structures. A range of piezopolymer sensors where used, varying in their dimensions, their capacitance and the electrode coating material. Sensors were tested in the surface-attached and embedded formats on composite sandwich laminates. Specimens were tested under three-point bending configuration to measure both the sensor voltages and the generated laminate strains. The electromechanical sensitivity performance with respect to frequency and strain amplitude were the key performance parameters investigated.

Conclusions, of a practical nature, were extracted concerning the appropriate type of sensor for embedding applications as well as the parameters affecting the sensitivity and efficiency of the devices to perform as both strain gauges and energy-harvesting devices. The main conclusions were as follows:

1. It is possible to calibrate small PVDF sensor patches as dynamic strain gauges. The measured sensitivity approaches the expected value, but only when the strain field around the calibration gauges and the PVDF sensors are sufficiently equivalent. In this sense a calibration on a complex sandwich panel section is not ideal. Further calibration will be required on ASTM standard tensile coupons. The preliminary results are, nevertheless, satisfactory.
2. Bonding of PVDF to the composite layer must be directly applied: even a thin layer of protection coating on the sensor (Mylar) results in hysteretic strain-voltage behaviour. This hysteresis manifests itself as an-out-of-phase oscillation of the generated voltage as a function of the applied periodic excitation. We conjecture that this is due to viscoelastic effects at the relatively thick interface of viscoelastic Mylar layer between the composite laminate and the piezo-film.
3. Prior to embedding a sensor in the composite laminate the compatibility of the sensor coating material and the matrix system should be investigated. It was shown that embedding a copper-nickel coated sensor (Type 2) with the current epoxy system results in a pronounced artificially created delamination debonding (inter layer separation) area.
4. The performance of the PVDF devices to generate voltage appeared to be insensitive or slightly improved when the frequency or the load of the excitation was increased beyond 1Hz and when suitable input measuring impedance is applied.
5. The measured sensitivity of the larger PVDF sensors appears to be lower than the analytically expected values. However, simple surface applications of the sensors on the composite structure presented small deviations from the theoretically expected values. On the other hand, embedding a sensor through the thickness of the composite laminate, especially when folded, results in a complex intralaminar strain field and this is, most probably, different from the strain measured on the surface under simple local conditions.

6. With regards to the fabrication methodology and its repeatability, a pair of nominally identical specimens tested presented similar trends with moderate differences (within explainable experimental and test condition differences) in the measured sensitivity values.
7. The application of a Copper Nickel coating sensor of 56μm thickness, on the surface of the thick sandwich composite structure resulted in the generation of high voltage ranges, up to 12 Volts peak-to-peak at less than 500 μstrain. The performance of PVDF devices can potentially provide the requested voltage for supplying an energy harvesting circuit at voltage levels of 3-6 volts, which are satisfactory for commercially-available electronic energy harvesting rectification circuits.

8. References

[1] W. J. Elspass, J. Kunzmann, M. Flemming and D. Baumann, "Design,manufacturing and verification of piezoceramics embedded in fiber-reinforced thermoplastics," in *Smart Structures and Integrated Systems,Proceedings of SPIE*, 1995.

[2] N. W. Hagood, E. F. Crawley, J. d. Luis and E. H. Anderson, "Development of integrated components for control of intelligent structures," in *Smart materials structures, and mathematical issues, U.S. Army Research Office Workshop,pp.80-104*, Blacksburg, VA, USA, Sep. 1988.

[3] S. Mall and T. L. Hsu, "Electromechanical fatigue behavior of graphite/epoxy laminate embedded with piezoelectric actuator," *Smart Materials and Structures,* vol. 9, no. 1, p. 78-84, 2000.

[4] J. Warkentin and F. Crawley, "Embedded electronics for intelligent structures," in *Proc. AIAA/AHS/ASME/ASCE/ASC 32nd Structures, Structural Dynamics and Materials Conf.*, Baltimore, MD, 1991.

[5] D. Shukla and A. Vizzini, "Interlacing for improved performance of laminates with embedded devices," *Smart Materials and Structures,* vol. 5, p. 225-229, 1996.

[6] J. Hansen and A. Vizzini, "Fatigue Response of a Host Structure with Interlaced Embedded Devices," *Journal of intelligent material systems and structures,* vol. 11, p. 902-909, 2000.

[7] F. Bellan, A. Bulletti, L. Capineri, L. Masotti, G. G. Yaralioglu, F. L. Degertekin, B. Khuri-Yakub, F. Guasti and E. Rosi, "A new design and manufacturing process for embedded Lamb waves interdigital transducers based on piezopolymer film," *Sensors and Actuators A,* vol. 123–124, p. 379–387, 2005.

[8] *Acellent Technologies Inc, 562 Weddell Drive, Suite 4, 94089 Sunnyvale, CA, USA.*

[9] E. F. Crawley and J. De Luis, "Use of piezoelectric actuators as elements of intelligent structures," *AIAA Journal,* vol. 25, p. 1373–85, 1987.

[10] W. T. Chow and M. J. Graves, "Stress analysis of a rectangular implant in laminated composites using 2-D and 3-D finite elements," in *Proc.AIAA/AHS/ASME/ASCE/ASC 33rd Structures, Structural Dynamics and Materials Conferences*, Dallas, TX, 1992.

[11] C. Caneva, I. M. De Rosa and F. Sarasini, "Acoustic Emission Monitoring of Flexurally Loaded Aramid/Epoxy Composites by Embedded PVDF Sensors," *Journal of Acoustic Emission,* vol. 25, pp. 80-91, 2007.

[12] M. Melnykowycz and A. Brunner, "The performance of integrated active fiber composites in carbon fiber laminates," *Smart Materials and Structures,* vol. 20, no. 7, p. art. no. 075007, 2011.

[13] A. Bronowicki, L. McIntyre, R. Betros and G. Dvorsky, "Mechanical validation of smart structures," *Smart Materials and Structures,* vol. 5, p. 129-139, 1996.

[14] S. Mall and J. Coleman, "Monotonic and fatigue loading behavior of quasisotropic graphite/epoxy laminate embedded with piezoelectric sensor," *Smart Materials and Structures,* vol. 7, p. 822-832, 1998.

[15] M. Yocum, H. Abramovich, S. Grunwald and A. Mall, "Fully reversed electromechanical fatigue behavior of composite laminate with embedded piezoelectric actuator/sensor," *Smart Materials and Structures,* pp. 556-564, 2003.

[16] H.-Y. Tang 'RAY', C. Winkelmann, W. Lestari and V. Saponara, "Composite Structural Health Monitoring Through Use of Embedded PZT Sensors," *Journal of intelligent materials systems and structures,* vol. 22, p. 739-755, 2011.

[17] K. Schaah, P. Rye and S. Nemat-Nasser, "Optimization of Sensor Introduction into Laminated Composites," in *SEM Annual Conference and Exploitation on Experimental and Applied Mechanics*, 2007.

[18] F. Ghezzo and S. Nemat-Nasser, "Effects of embedded SHM sensors on the structural integrity of glass fiber/epoxy laminates under in-plane loads," in *SPIE*, San Diego, 2007.

[19] E.Gutiérrez, S. Mainetti and E. Ruotolo, "D02.01 Report on feasibility of piezo-polymer energy harvesting systems.," Joint Research Center,JRC77812, Ispra, Italy, 2012.

[20] "Easy Composites," [Online]. Available: http://www.easycomposites.co.uk/.

[21] "Piezo Film Sensors," Measurement Specialties, [Online]. Available: http://www.meas-spec.com/.

[22] S. Mainetti, E. Ruotolo and E.Gutiérrez, "D02.02. Report on manufacturing feasibility of embedded piezothermoplastic polyvinylidene difluoride (PVDF) systems," Joint Research Center,JRC77815, Ispra, Italy, 2012.

[23] S. Butler, M. Gurvich, A. Ghoshal, G. Welsh, P. Attridge, H. Winston, M. Urban and N. Bordick, "Effect of embedded sensors on interlaminar damage in composite structures," *Intelligent materials systems and structures,* vol. 22, no. 16, p. 1857–1868, 2011.

[24] Y. Huang and S. Nemat-Nasser, "Structural Integrity of Composite Laminates with Embedded Micro sensors," in *Sensor Systems and Networks: Phenomena,Technology, and Applications for NDE and Health Monitoring,Proc. Of SPIE*, 2007.

European Commission
EUR 26341 EN – Joint Research Centre – Institute for the Protection and Security of the Citizen

Title: Objective 2: Conduct Experimental Activities on Performance of Sensor-Equipped Composite Elements

Author(s): N.A. Chrysochoidis, S. Mainetti, E. Ruotolo, E. Gutiérrez

Luxembourg: Publications Office of the European Union

2013 – 54 pp. – 21.0 x 29.7 cm

EUR – Scientific and Technical Research series – ISSN 1831-9424

ISBN 978-92-79-34691-0

doi:10.2788/41247

Abstract

In this report we present the basic principles of our investigations for embedding sensors and energy-harvesting devices in sandwich composite structures. A range of piezopolymer sensors where used, varying in their dimensions, their capacitance and the electrode coating material. Sensors were tested in the surface-attached and embedded formats on composite sandwich laminates. Specimens were tested under three-point bending configuration to measure both the sensor voltages and the generated laminate strains. The electromechanical sensitivity performance with respect to frequency and strain amplitude were the key performance parameters investigated. Primary conclusions, of a practical nature, were extracted concerning the appropriate type of sensor for embedding applications as well as the parameters affecting the sensitivity and efficiency of the devices to perform as both strain gauges and energy-harvesting devices.

LB-NA-26341-EN-N

As the Commission's in-house science service, the Joint Research Centre's mission is to provide EU policies with independent, evidence-based scientific and technical support throughout the whole policy cycle.

Working in close cooperation with policy Directorates-General, the JRC addresses key societal challenges while stimulating innovation through developing new standards, methods and tools, and sharing and transferring its know-how to the Member States and international community.

Key policy areas include: environment and climate change; energy and transport; agriculture and food security; health and consumer protection; information society and digital agenda; safety and security including nuclear; all supported through a cross-cutting and multi-disciplinary approach.

Publications Office

ISBN 978-92-79-34691-0